

**FR-8091**

**Modifications to and Preliminary Results for the ADIT  
System**

**G.V. Trunk  
J.D. Wilson  
B.H. Cantrell  
J.J. Alter  
F.D. Queen**

**April 19, 1977**

**Naval Research Laboratory**

REPORT DOCUMENTATION PAGE		READ INSTRUCTIONS BEFORE COMPLETING FORM
1. REPORT NUMBER NRL Report 8091	2. GOVT ACCESSION NO.	3. RECIPIENT'S CATALOG NUMBER
4. TITLE (and Subtitle) MODIFICATIONS TO AND PRELIMINARY RESULTS FOR THE ADIT SYSTEM		5. TYPE OF REPORT & PERIOD COVERED Interim report on one phase of a continuing NRL problem
		6. PERFORMING ORG. REPORT NUMBER
7. AUTHOR(s) G. V. Trunk, J. D. Wilson, B. H. Cantrell, J. J. Alter, and F. D. Queen		8. CONTRACT OR GRANT NUMBER(s)
9. PERFORMING ORGANIZATION NAME AND ADDRESS Naval Research Laboratory Washington, D. C. 20375		10. PROGRAM ELEMENT, PROJECT, TASK AREA & WORK UNIT NUMBERS NRL Problems R02-54 and R12- 012 ZF 12-15-001 SF12-141-41B 62712N
11. CONTROLLING OFFICE NAME AND ADDRESS Department of the Navy Office of Naval Research Arlington, Va. 22317		12. REPORT DATE April 19, 1977
		13. NUMBER OF PAGES 45
14. MONITORING AGENCY NAME & ADDRESS (if different from Controlling Office)		15. SECURITY CLASS. (of this report) Unclassified
		15a. DECLASSIFICATION/DOWNGRADING SCHEDULE
16. DISTRIBUTION STATEMENT (of this Report)  Approved for public release; distribution unlimited.		
17. DISTRIBUTION STATEMENT (of the abstract entered in Block 20, if different from Report)		
18. SUPPLEMENTARY NOTES		
19. KEY WORDS (Continue on reverse side if necessary and identify by block number) ADIT Detectors Radar integration Tracking		
20. ABSTRACT (Continue on reverse side if necessary and identify by block number) The basic system philosophy of the automatic detection and integrated tracking (ADIT) system has been reviewed. The only change to the detection system has been the addition of a merging circuit to reduce target splits. The tracking program has been modified to improve tracking performance. Included in the new tracking program are dual clutter map, new tracking filter, new correlation logic based on track quality, automatic bias correlation between radars, sector censoring capability, and a new program control.  (Continued)		

20. ABSTRACT: (Cont'd)

Analysis of recorded data showed that the detection system works as anticipated, detecting the targets and limiting the false alarms to a manageable number. Analysis of tracking data yielded the following conclusions: (a) detections, not tracks, should be merged, (b) tracks should be initiated with at least three detections, (c) a dual clutter map should be used, (d) the SPS-12 and SPS-39 supply an equal number of detections, (e) bias correction procedures work when the azimuth bias is less than the normal track correlation region, (f) typical errors between measured and predicted positions are 0.20 n.mi. and  $0.5^\circ$ , and (g) the turn detector enables the tracking filter to follow maneuvering targets.

## CONTENTS

INTRODUCTION .....	1
BASIC SYSTEM PHILOSOPHY .....	2
AUTOMATIC DETECTION .....	4
SPS-12 Detector .....	5
SPS-12 Detection Results .....	6
SPS-39 Detector .....	10
SPS-39 Detection Results .....	10
Detector Summary .....	16
TRACKING SYSTEM .....	16
Tracking Overview .....	16
Dual Clutter Map .....	18
Tracking Filter .....	19
Correlation Logic .....	21
Radar Bias Correction .....	22
Input Structure .....	23
Output Structure .....	23
Alphameric Display .....	30
Status Parameters .....	31
TRACKING RESULTS .....	32
Experiment 1 (SPS-12 only) .....	32
Experiment 2 (SPS-39 only) .....	33
Experiment 3 (SPS-12 and SPS-39) .....	33
Experiment 4 (Poor Initiation) .....	34
Experiment 5 (Improved Initiation) .....	35
Tracking Accuracy .....	36
Bias Correction .....	40
SUMMARY .....	41
REFERENCES .....	42

# MODIFICATIONS TO AND PRELIMINARY RESULTS FOR THE ADIT SYSTEM

## INTRODUCTION

During fleet exercises in the 1960's, it was demonstrated that many targets were never detected by radar operators even though post test analysis of video recordings of the radar data revealed that the radar return from targets was present in the raw video. Among the reasons operators missed targets were operator fatigue; collapsing of upper beams of the 3D radar onto a plan-position indicator (PPI) display; and rain, land, and sea clutter. Thus, to improve its surveillance capability the Navy decided to associate automatic detection and tracking (ADT) systems with its radars. Specifically, the SPS-48C and the radar video processor (RVP) for 2D radars have been approved for fleet operation.

On board most naval combat vessels, there are two kinds of surveillance radars: 2D and 3D. To better use the information aboard the vessel, the radar data from different radars should be integrated to yield a single track file. The benefits of such a system would be increased data rate, quicker track initiations, increased track life, and on-line redundancy. Consequently, in the Spring of 1973, NRL started work on an automatic detection and integrated tracking (ADIT) system [1-4] that performs radar integration. Generally, automatic detectors are associated with the 2D SPS-12 and the 3D SPS-39, and the centroided detections are integrated into a single track file in a minicomputer.

Somewhat later, the Applied Physics Laboratory (APL) embarked on a similar program, which resulted in the SYS-1-D system [5]. The SYS-1-D system adopted the NRL system philosophy (merging detections) and uses several other features that were generated by the ADIT program. While the NRL ADIT system is a 6.2 research program, the APL SYS-1-D system is a 6.4 program designed for fleet introduction. Currently, the SYS-1-D system is scheduled to be tested in the fleet in early 1978.

This report describes the changes to the ADIT system that have been made in the last year and gives some preliminary results quantifying the performance of the ADIT system. The basic system philosophy is reviewed in the next section, which describes how the SPS-39 is used in a lobe filler mode and reports elevation only on designated targets.

The parameter settings that are used with the modified generalized sign test processor [1,6] and a description of the new beam splitter that was built are given. Photographs of a PPI with raw video and detected video are shown, and detection results are stated.

An overview of the tracking system and a description of the various modifications made to the tracking system are given. Included in the new tracking program are a dual clutter map,

---

Manuscript submitted December 3, 1976.

a new tracking filter, a new correlation logic based on track quality, an automatic bias correction between radars, a sector censoring capability, and a program control to facilitate parameter changes and to expand output capabilities.

Preliminary results quantifying system performance are discussed. Performance measures include effectiveness of the dual clutter map, effectiveness of radar integration for increasing track life, and tracking accuracy.

Conclusions and future work are discussed in the final section.

## BASIC SYSTEM PHILOSOPHY

The basic system concept is shown in Fig. 1. The SPS-12 radar is a 2D radar that operates in its normal mode. The SPS-39 radar is a 3D radar that operates in a modified mode, using two lower beams to fill in the multipath nulls of the SPS-12. Automatic target-detection systems are associated with each radar. The ATD systems not only detect targets but also estimate the azimuthal position of the target and inhibit multiple detections from a target. The detections are transmitted to the minicomputer via a direct memory access (DMA) channel. The minicomputer performs the system tracking, accepting detections from both radars and integrating (combining) them into a single track file. The tracking system is monitored by the synthetic video display — a color TV which displays target status (firm, tentative, detecting radars, under elevation scan, or being handed off) — the alphanumeric display, and the system status parameters. The radar operator interacts with the system via the alphanumeric display. Some of the operator requests include track information on various targets, tracks identified by specified parameters (high velocity, azimuth sector, etc.), and demands for height on selected targets. When a height demand is received, the tracking computer calculates the next update time for the SPS-39, sends a message at this time to the SPS-39 to stop its search pattern, and performs several elevation scan patterns. The elevation of the selected target is then sent back to the tracking computer.

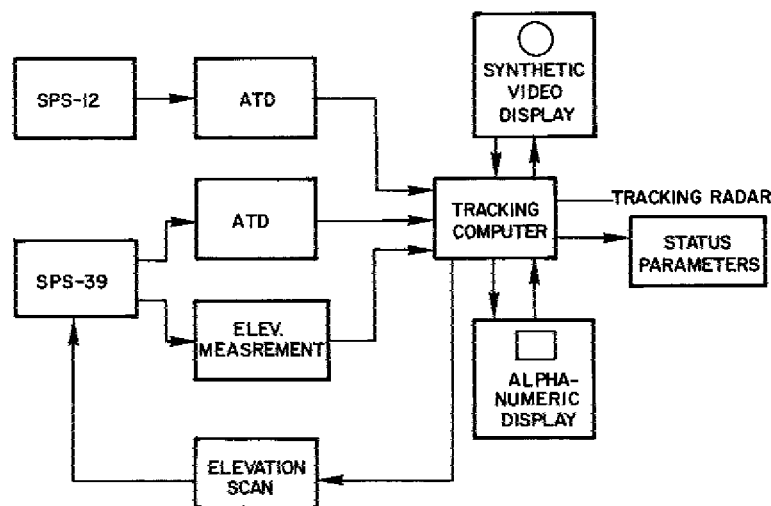


Fig. 1 - Basic system concept for radar integration

The SPS-12 is an L-band search radar. The coverage pattern for the SPS-12 located 50 m (166 ft) above water (on the roof of building 75 at the Chesapeake Bay Division of NRL) was calculated using Blake's computer program [7] and is shown in Fig. 2. The familiar lobing pattern due to multipath is present. If one tried to perform automatic tracking with this radar or any other naval 2D radar, one would encounter severe fading conditions that make it difficult to maintain tracks [8,9].

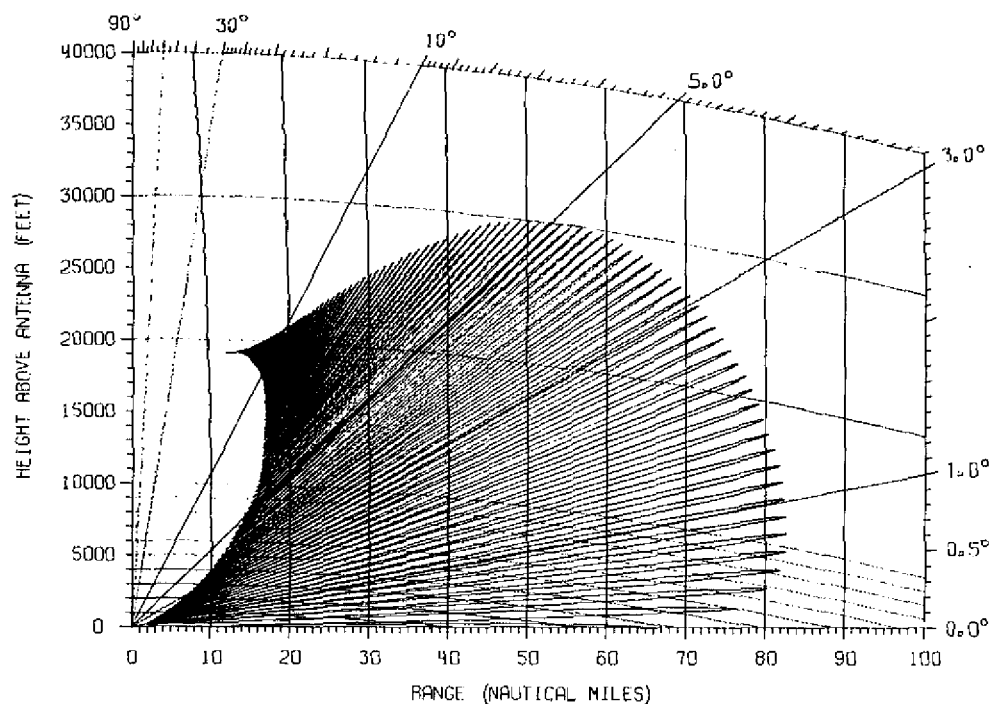


Fig. 2 - Antenna pattern of the SPS-12 radar with an antenna height of 50 m (166 ft) and a free-space range of 42.5 n.mi. (1 ft = 0.3048 m)

To reduce the fading problem, two lower beams of the SPS-39 are used to fill in the nulls of the SPS-12. If one transmits only on two beams and obtains 8 hits with the beam pointed at  $3.3^\circ$  and 15 hits with the beam pointed at  $1.8^\circ$ , one obtains the composite coverage pattern shown in Fig. 3. This composite pattern is obtained by plotting the farthest detection range of the radars (the SPS-12 and the two beams of the SPS-39) at each elevation angle. Comparing Figs. 2 and 3, one should note that between  $1^\circ$  and  $5^\circ$  very few nulls exist in the composite pattern, and that below  $1^\circ$  the nulls are narrower and not as deep for the composite pattern.

Before proceeding to the principal subject of this report, the method of integration will be discussed briefly. There are several possible methods of radar integration — the following ones are the most frequently mentioned:

1. Detections from both are radars used to initiate and update tracks
2. Track initiated on one radar and detections from both radars are used to update tracks
3. Tracks from both radars are merged to yield a single track

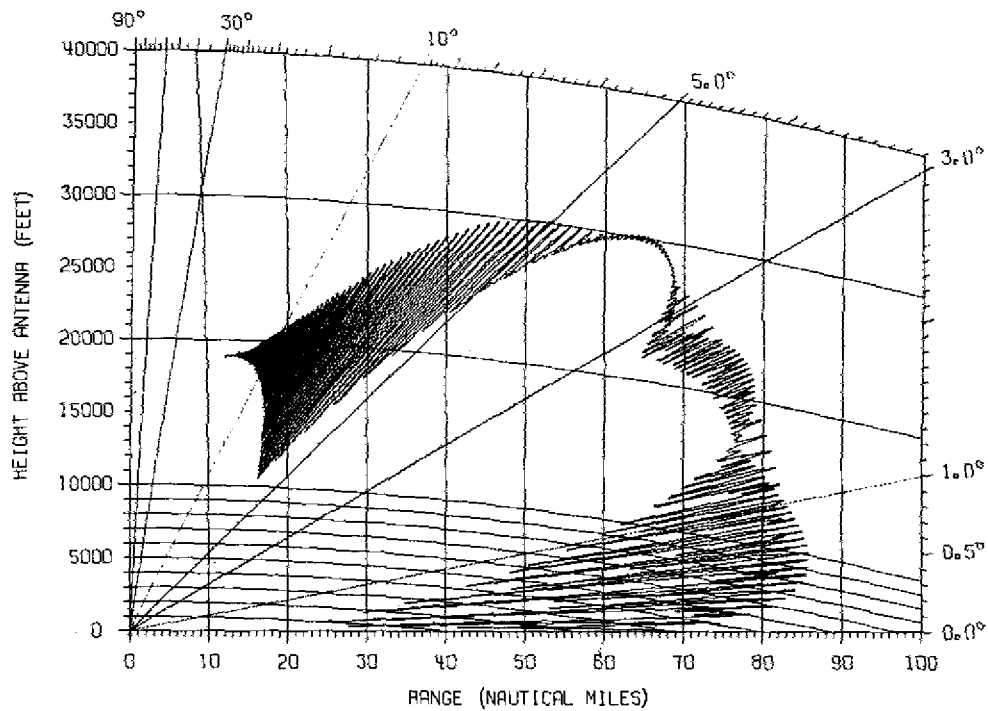


Fig. 3 — Composite antenna pattern for the SPS-12 and SPS-39 radars. The antenna height is 50 m (166 ft), the free-space range of the SPS-12 is 42.5 n.mi., the free-space range of the  $1.8^\circ$  elevation beam of the SPS-39 is 77 n.mi., and the free-space range of the  $3.3^\circ$  elevation beam is 68.6 n.mi. (1 ft = 0.3048 m)

4. One of the radars is chosen using a specified criterion; i.e., highest quality or earliest track.

Since the first method contains the maximum information, since all other methods can be considered to be special cases of it, and since both our radars are stabilized and have comparable accuracy, the first method was used to integrate the radars. The problem with this method is that care must be taken so that poor radar data (for instance, from a jammed radar) do not corrupt good radar data. It should be noted that for other radar suites, such as the SPS-48 and SPS-40, this method should not be used.

#### AUTOMATIC DETECTION

The ATD systems are discussed in a previous report [1]. However, several of the adjustable parameters for the ATD systems have been set to new operational values. Furthermore, a new merging circuit has been built to reduce target splits. These changes are discussed in the following paragraphs.

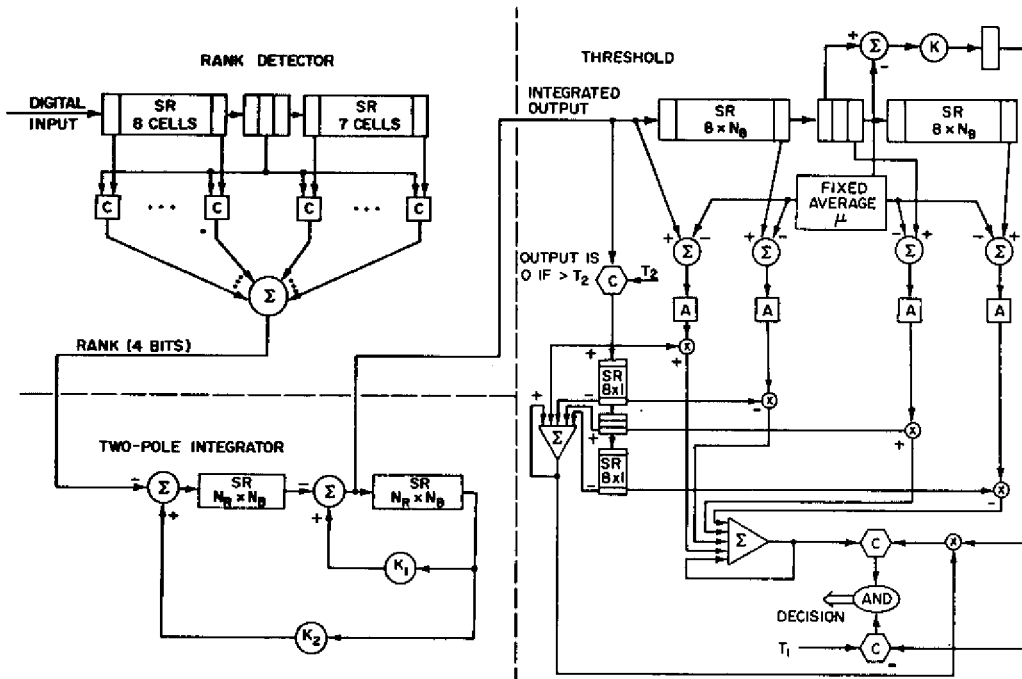


Fig. 4 — Block diagram of the MGST processor [6]

**SPS-12 Detector**

The detector (modified generalized sign test (MGST) processor) for the SPS-12 is shown in Fig. 4. As shown in Fig. 4 by the dashed lines, the processor can be divided into three parts: a rank detector, a two-pole integrator, and a threshold (decision process). Basically, the detector works as follows: Let  $x_{ij}$  be the  $i$ th returned pulse in the  $j$ th range cell. The rank detector computes the rank  $R_{ij}$  by making pairwise comparisons:

$$R_{ij} = \sum_k C(x_{ij} - x_{ik}) \tag{1}$$

where

$$C(x) = \begin{cases} 1, & x > 0 \text{ or } x = 0 \text{ and } k - j \text{ odd} \\ 0, & x < 0 \text{ or } x = 0 \text{ and } k - j \text{ even} \end{cases}$$

and the  $k$  summation is over the  $L$  range cells surrounding the  $j$ th cell. The two-pole integrator calculates the weighted rank sum

$$Z_{ij} = \sum_{k=0}^{\infty} h_k R_{i-k,j} \tag{2}$$

where  $h_k$  is the impulse response of the two-pole filter. A target is declared when the integrated output exceeds two thresholds. The first threshold is fixed (equals  $\mu + T_1/K$  from Fig. 4) and yields a  $10^{-6}$  probability of false alarm  $P_{fa}$  when the reference samples are independent and identically distributed. The second threshold is adaptive and maintains a low  $P_{fa}$  when the reference samples are correlated. The device uses the mean deviate estimate where extraneous targets in the reference cells have been censored to estimate the standard deviation of the correlated samples.

The original detector settings produced too many false alarms in clutter. Consequently, we revised these settings by performing analytic calculations (Ref. 6, App. II) and experimental trial-and-error tests. The new values are as follows:

$$\begin{aligned} K_1 &= 1.875 \\ K_2 &= 1.8828 \\ \bar{K} &= .1172 \\ \mu &= 832 \\ T_1 &= 73.5 \\ T_2 &= 2032 \end{aligned}$$

Note that  $T_2 = 2032$  effectively disables the extraneous target censoring. While these revised parameter values reduced the number of false alarms, there remained a tendency for multiple reports, either in range or azimuth, from clutter. This was thought to be a result of the interaction of the nonhomogeneous clutter, radar pulse width, rank detector, and the adaptive thresholding. To remedy this situation, an  $M$ -out-of- $N$  integrator-stretcher was built and is shown in Fig. 5. The output of the MGST processor, either a 0 or 1, is an input to an integrate-and-dump circuit. After accumulating  $N$  pulses, switches  $A$  are closed (simultaneously switches  $B$  are opened); and the sum is compared to  $M$ , a target being declared if the sum equals or exceeds  $M$ . These detections are then stretched  $LN$  pulses. Because the present values for the SPS-12 are  $N = 4$  and  $L = 8$ , any two targets within approximately  $4.0^\circ$  (angle radar scans through during transmission of  $LN = 32$  pulses) will be merged into a single target report if they are in the same range cell. Furthermore, the inhibiting circuitry originally associated with the beam splitting circuit [Ref. 1, Fig. 18] was added to the merging circuit so that targets in adjacent range cells separated by less than  $4^\circ$  will also be merged.

It should be noted that this merging circuit is required by the fact that the system is operating in land clutter without an MTI. If the radar had either an MTI or were operating in an ocean environment, the merging circuit should not be used because it decreases the resolution capability of the radar system. Specifically, problems occur for the extremely important case of the incoming wave of targets; i.e., closely spaced targets are not resolved.

### SPS-12 Detection Results

The hardware implementation of the MGST processor was checked by simultaneously recording the input data and the detections reported by the MGST processor. The input data, specifically the median of every three azimuth pulses, quantized to a zero or one, is plotted in a B-scope presentation in Fig. 6. The area covered is approximately 10 n.mi. by  $25^\circ$  ( $3$  to  $13$  n.mi.,  $73^\circ$  to  $98^\circ$ ). The near-range return is land clutter from the sidelobes, the low return is from the Chesapeake Bay and Choptank River, the targets in the Bay are ships and buoys, and the solid return is from land.

These same data are shown in Fig. 7 where the threshold crossings from the MGST processor have been added. The video return has been quantized to three levels (blank is low return,  $Y$  is moderate return, and  $X$  is a high return) and threshold crossings are denoted by  $D$ 's. There is a  $20\text{-}\mu\text{s}$  delay in the processor; i.e., time for pulses to pass through all the shift registers and logic circuits. Consequently, threshold crossings are reported 20 range cells behind the target, and they also lag in azimuth. There are seven threshold crossings, corresponding to six ships in the Chesapeake Bay and one from clutter. The threshold crossing corresponding to the

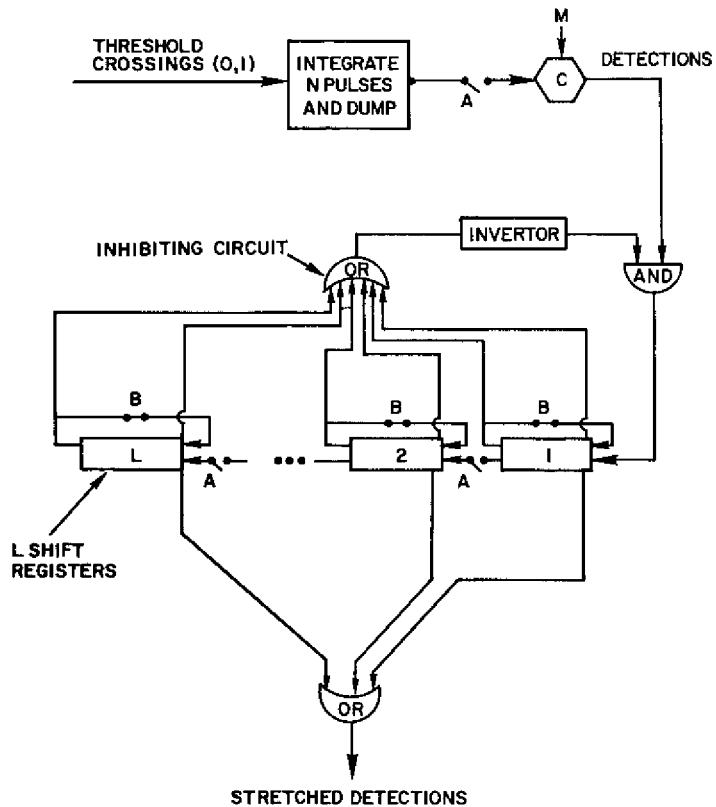


Fig. 5 — Block diagram of the  $M$ -out-of- $N$  integrated-stretcher

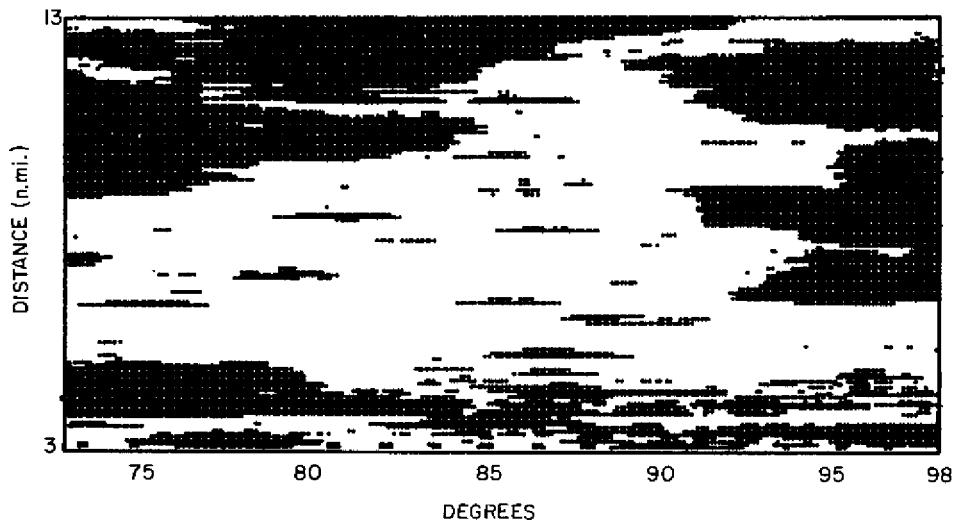


Fig. 6 — Quantized B-scope presentation

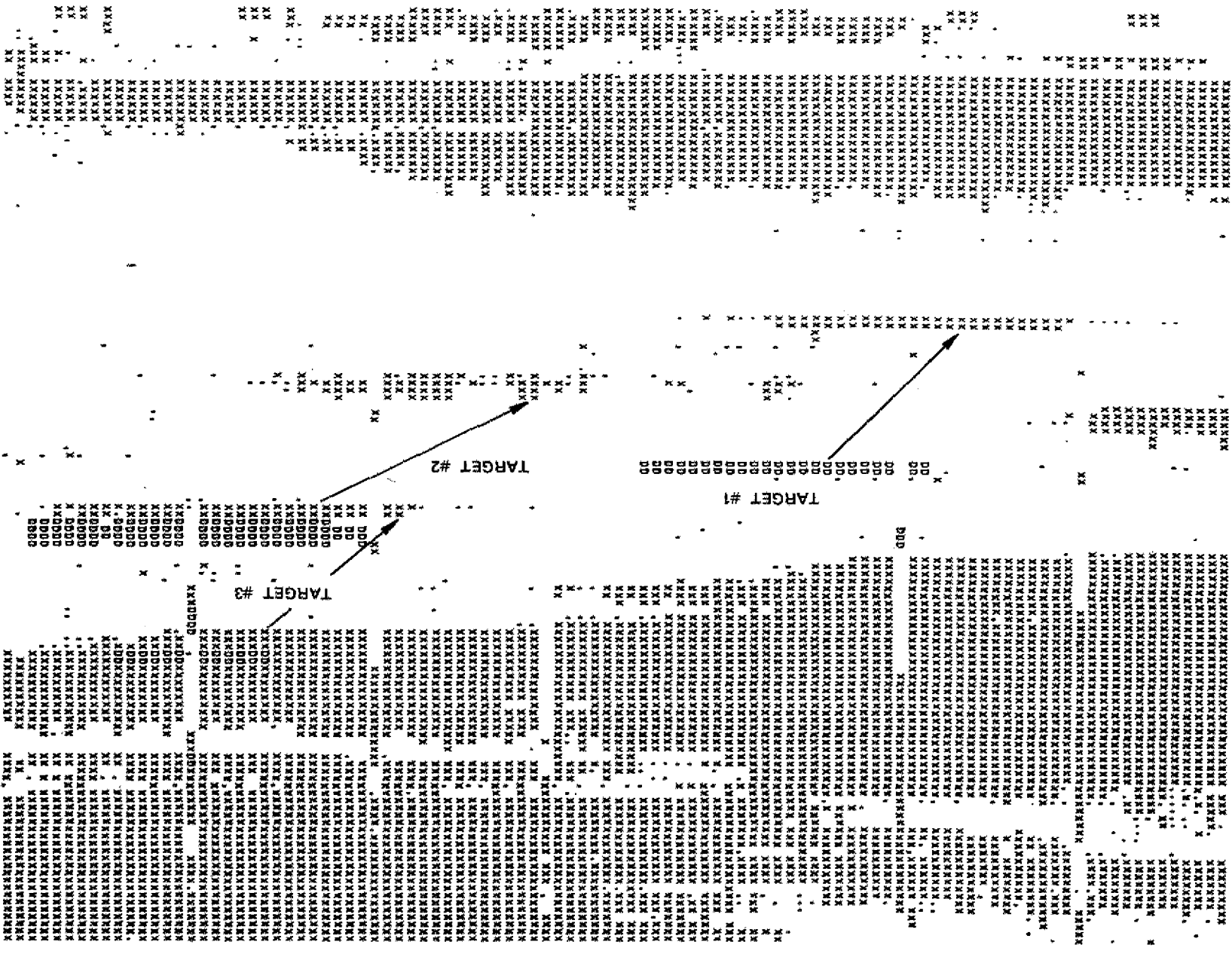


Fig. 7 — Quantized B-scope presentation with detections from ATD



sixth target is very short. This is because the integrated return from the fourth target in the MGST processor is only five range cells from the sixth target, falls in the reference cells, of the sixth target and raises the adaptive threshold. Thus, for a large portion of the time, the fourth target is masking the sixth target.

There are also several one-pulse threshold crossings. However, examination of the data reveals that the data are shifting several range cells. This problem was traced to the recording hardware, and, therefore, had no impact on the detections reported to the tracking system. Also, of note is the fact that there are no detections from the solid land clutter; there is one clutter detection off a peninsula.

Because false alarms are caused principally by clutter, the statistical properties of the clutter are very important. Some A-scope presentations are shown in Figs. 8 and 9. The three sweeps in Fig. 8 correspond to successive PRF's and the three sweeps in Fig. 9 correspond to successive scans. While only minor changes are present in the pulse-to-pulse presentations, several major changes can be seen in the scan-to-scan presentations. Unfortunately, a detailed statistical analysis of the clutter data has not yet been completed.

### SPS-39 Detectors

There are three different detectors for the SPS-39: one for the lower beam where 15 pulses are integrated, one for the upper beam where 8 pulses are integrated, and one for the elevation scan where only one pulse is available. The detector for the lower beam is the MGST processor shown in Fig. 4. For the SPS-39, the parameters are as follows:

$$\begin{aligned} K_1 &= 1.75 \\ K_2 &= 0.7813 \\ \bar{K} &= 0.1406 \\ \mu &= 208 \\ T_1 &= 28.125 \\ T_2 &= 480 \end{aligned}$$

Similarly to the SPS-12, the thresholding crossings of the MGST processor for the SPS-39 are an input to the merging circuit shown in Fig. 5. The present values for the SPS-39 merging circuit are  $N = 4$ ,  $M = 3$ , and  $L = 4$ . Since  $NL = 16$ , all targets within a beamwidth are merged.

The rank detector for the upper beam of the SPS-39 is shown in Fig. 10 and the log-Rayleigh detector for the elevation scan is shown in Fig. 11. The parameter settings for the rank detector are  $M = 6$ ,  $N = 8$ , and  $K = 14$ . For the rank detector each detection is stretched four PRF's, and detections in adjacent range cells are inhibited. The parameter  $K$  in the log-Rayleigh detector is set by trail and error. Its value is now 64.0

### SPS-39 Detection Results

The raw video and the threshold crossings of the MGST processor, delayed by two scans, are shown in Figs. 12a and 12b, respectively. A manageable number (one that does not overwork tracking computer) of clutter returns is present. In the raw video, the presence of ducting (approximately at  $20^\circ$  and  $155^\circ$ ) should be noted. The detections in these areas are quite inconsistent, fluctuating on a scan-to-scan basis, and, consequently, a number of false tracks are generated. This problem will be investigated in the near future.

Fig. 9 — A-scope presentation of three successive scans

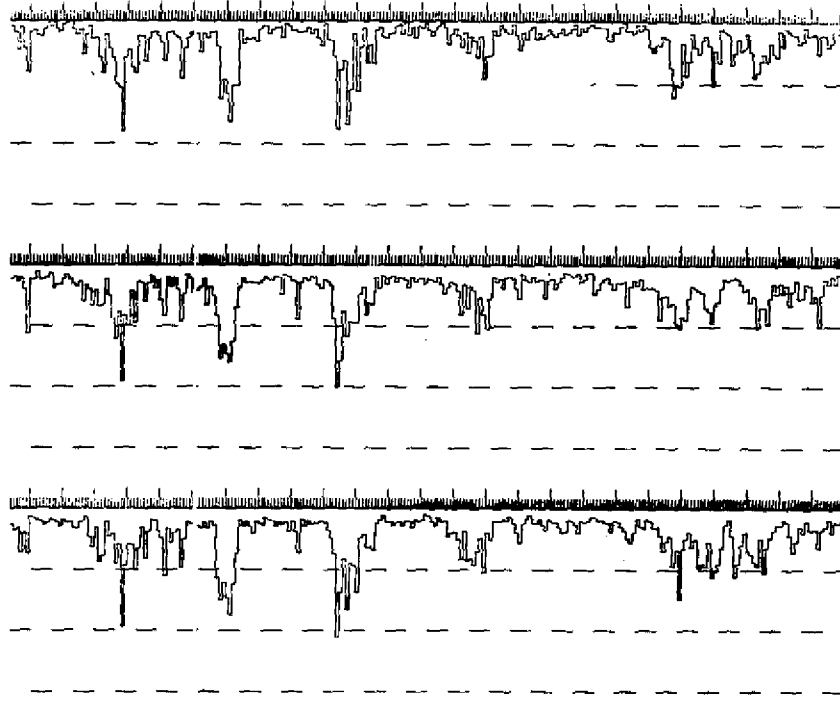
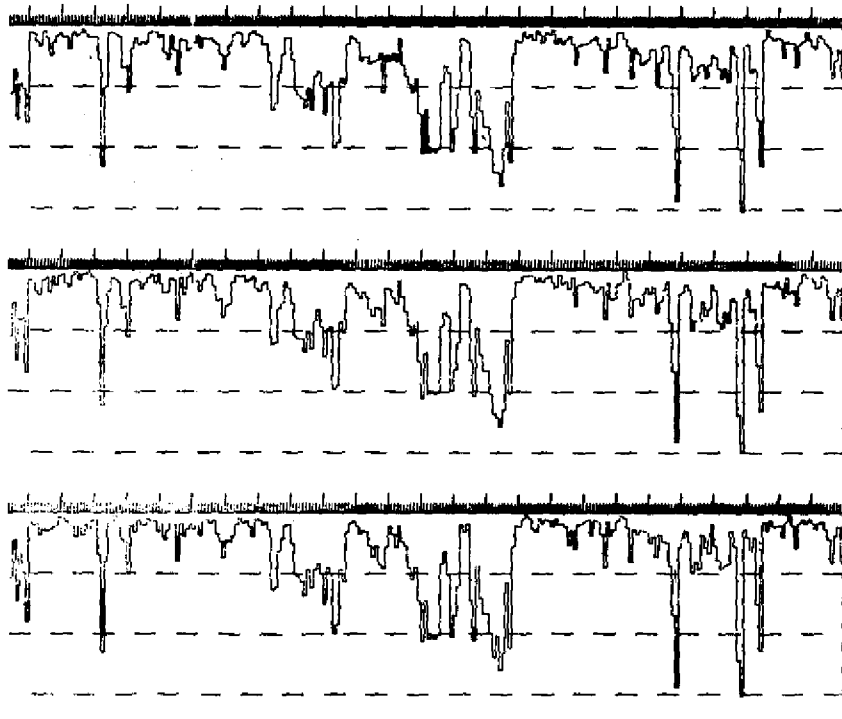


Fig. 8 — A-scope presentation of three successive PRFs



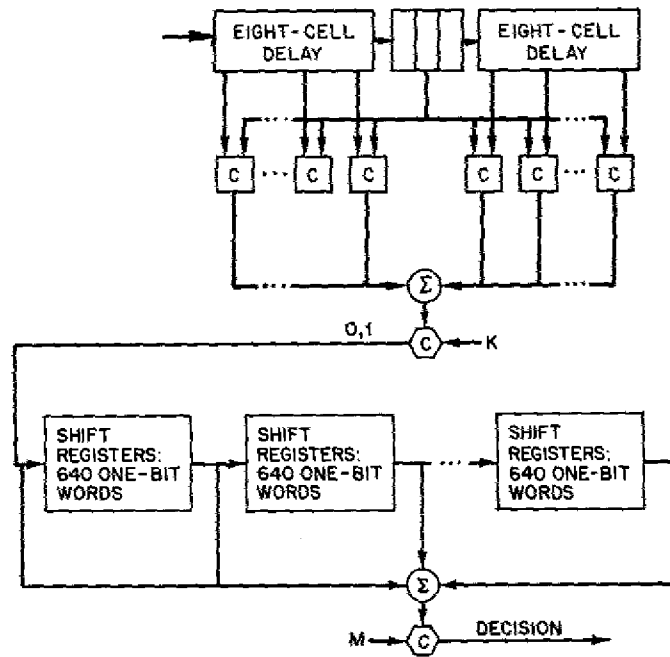


Fig. 10 — Nonparametric rank detector with a moving-window (*M*-out-of-*N*) integrator

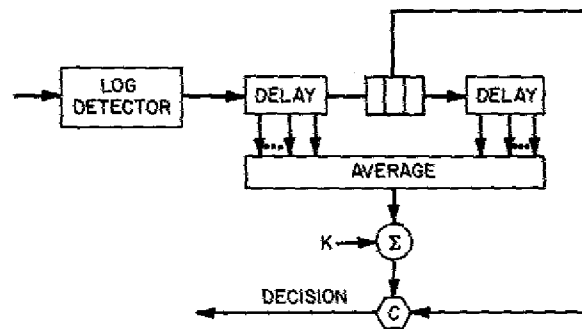
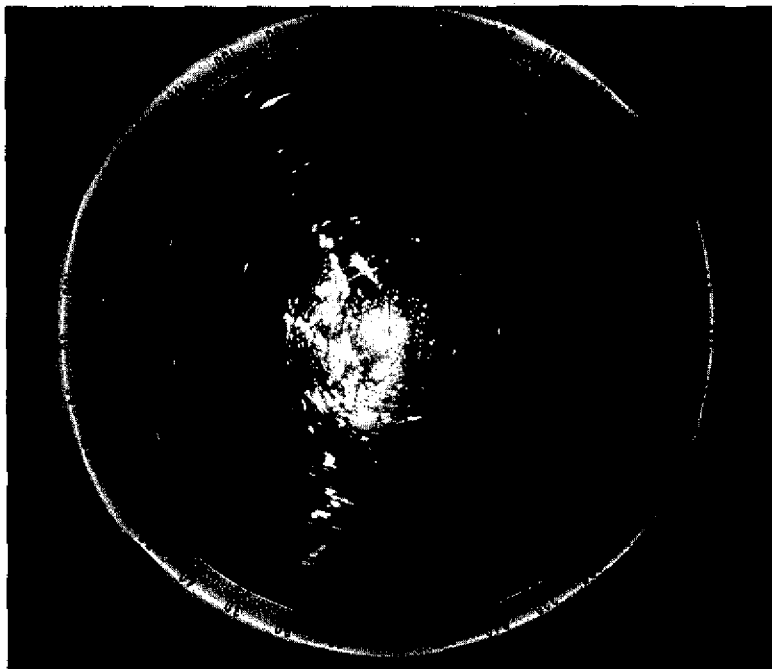


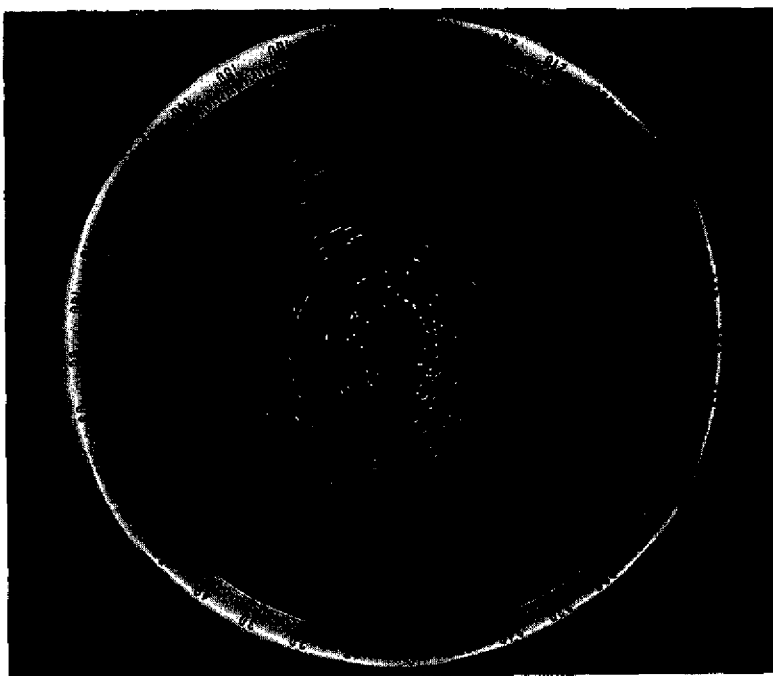
Fig. 11 — Log-Rayleigh detector for the elevation scan

Fig. 12 — (a) PPI presentation of SPS-39 raw video (b) PPI presentation of MGST processor using lower beam.

(b)



(a)



The effects of noise jamming can be seen in Figs. 13a and 13b. The MGST processor not only clears up the PPI presentation but also preserves the target detections. However, this was because the targets were stronger than the jamming. If the jamming were stronger, the PPI would be blank. The most effective ways of minimizing the effects of jamming are the use of low sidelobe antennas or sidelobe cancelers or both.

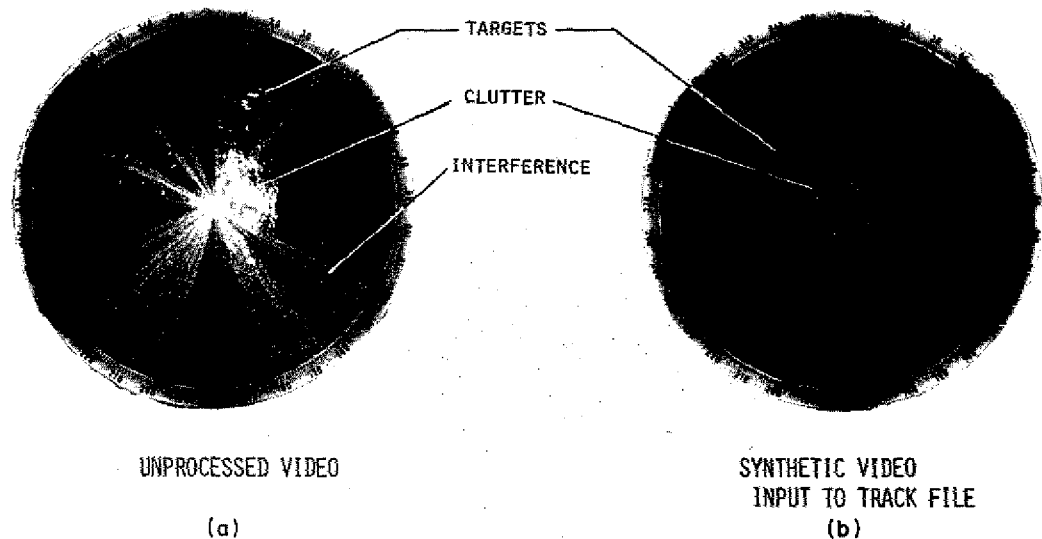


Fig. 13 — (a) PPI presentation of SPS-39 raw video with noise jamming. (b) PPI presentation of MGST processor in noise jamming.

The threshold crossings of the rank detector for the upper beam of the SPS-39 are shown in Fig. 14. There are many threshold crossings at near ranges. These are caused by the facts that the SPS-39 has poor elevation sidelobes and that the rank detector only yields a constant false alarm rate when the reference cells are independent and identically distributed, an assumption violated by the clutter correlation. Consequently, all detections within IR39U (2048 counts) are eliminated.

To compare results of the rank detector with the MGST processor, we used the data in Fig. 7 as input to a computer simulation of a rank detector. The threshold crossings of the rank detector with  $K = 14$ ,  $M = 20$ , and  $N = 30$  (this corresponds to a probability of false alarm less than  $10^{-7}$  in thermal noise) are shown in Fig. 15. There are approximately 25 threshold crossings. Because there are six ships present, the number of detections due to clutter has risen from 1 to 19. Thus, in correlated clutter, adaptive thresholding detectors must be used.

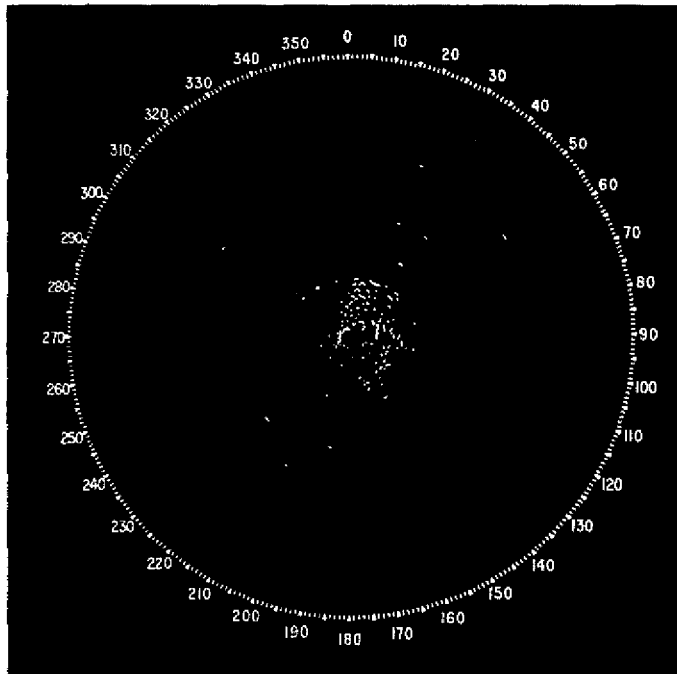


Fig. 14 — PPI presentation of the rank detector using the upper beam of the SPS-39 (Upper beam = 100 n.mi.)

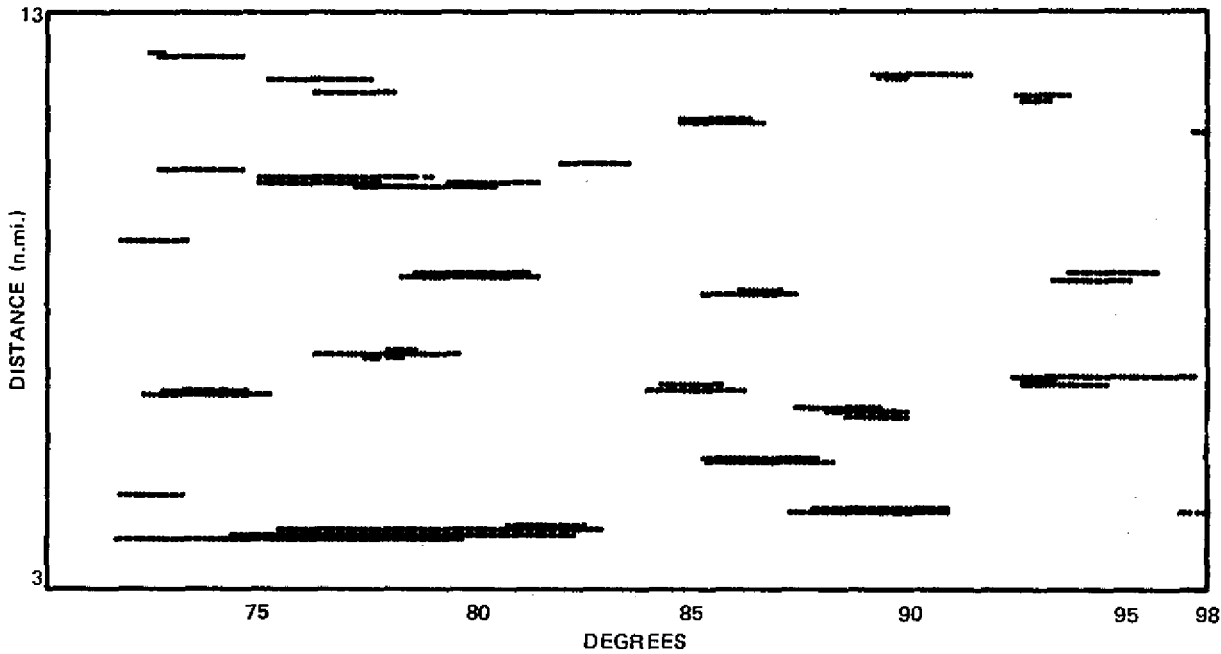


Fig. 15 — Threshold crossings of a rank detector ( $K = 14$ ,  $M = 20$ , and  $N = 30$ ) applied to data appearing in Fig. 7

### Detector Summary

It has been shown that the detectors work as anticipated — detecting the targets and limiting the false alarms to a small enough number that does not saturate the tracking computer. Also, it is necessary to have adaptive thresholding in clutter areas if one does not have an MTI. The MGST processor, which incorporates a nonparametric detector with adaptive thresholding, performs extremely well. However, the MGST processor is a complicated detector that was originally designed to operate without a radar operator performing control functions such as sectoring. Presently, we feel that the operator should have the capability of setting different thresholds in various sectors.

### TRACKING SYSTEM

The tracking system is discussed in detail in Ref. 2, and the changes to the system made in 1975, such as the new initiation scheme, new tracking filter, and new correlation method, are discussed in Ref. 4. The basic mode of operation is reviewed in the next section, and the modifications to the tracking program follow. Included in the new tracking program are a dual clutter map, a new tracking filter, a new correlation logic based on track quality, an automatic bias correction between radars, a sector censoring capability, and a program control to facilitate input changes and to expand output capabilities.

### Tracking Overview

The 360° of azimuth are divided into 64 equal-azimuth sectors. This sectoring enables correlation between tracks and detections to be done only in a local area and enables tracks to be easily updated with the oldest (in time) detections. The time sequence of operations is illustrated in Fig. 16 where scan times of 5.76 and 8.32 s have been assumed for the SPS-12 and SPS-39, respectively. The positions of the two radars are shown at  $t = 10$  s, and the time of the sector crossings by the radars are shown on the circumference of the circle. During the previous update, the choice was between updating sector 49 (with SPS-39 data) or updating sector 12 (with SPS-12 data). Since the sector crossing times were 9.34 and 9.42 s for sectors 12 and 49 respectively, the oldest sector in time, sector 12, was updated. After this sector was updated, the choice was between sector 13 (with SPS-12 data) and sector 49 (with SPS-39 data). The oldest sector data is then in sector 49; consequently, the sector was updated. The details involved in updating a track sensor will now be illustrated using sector 49 and SPS-39 data.

First, the clutter points three sectors in advance of the track sector are correlated (act of *trying* to associate) with the detections in that sector and in the adjacent sectors. The closest detection in the correlation region replaces the clutter point, and all other detections in the clutter correlation region are eliminated. In our case, the clutter points in sector 52 are correlated with the detections in sectors 51, 52, and 53. Then, since the SPS-39 radar is being updated, unused detections from the upper and lower beam detectors of the SPS-39 are merged into a single detection if they are identified as the same target. Next, the tracks are updated with the detections in four sectors (two sectors in advance of the track sector,\* and one sector behind the track sector). A series of passes, with different correlation region sizes, is made through the

\*Tracks are correlated with detections two sectors in advance because there is a delay in reporting detections; the report is made at the end of the detection, after it has been stretched.

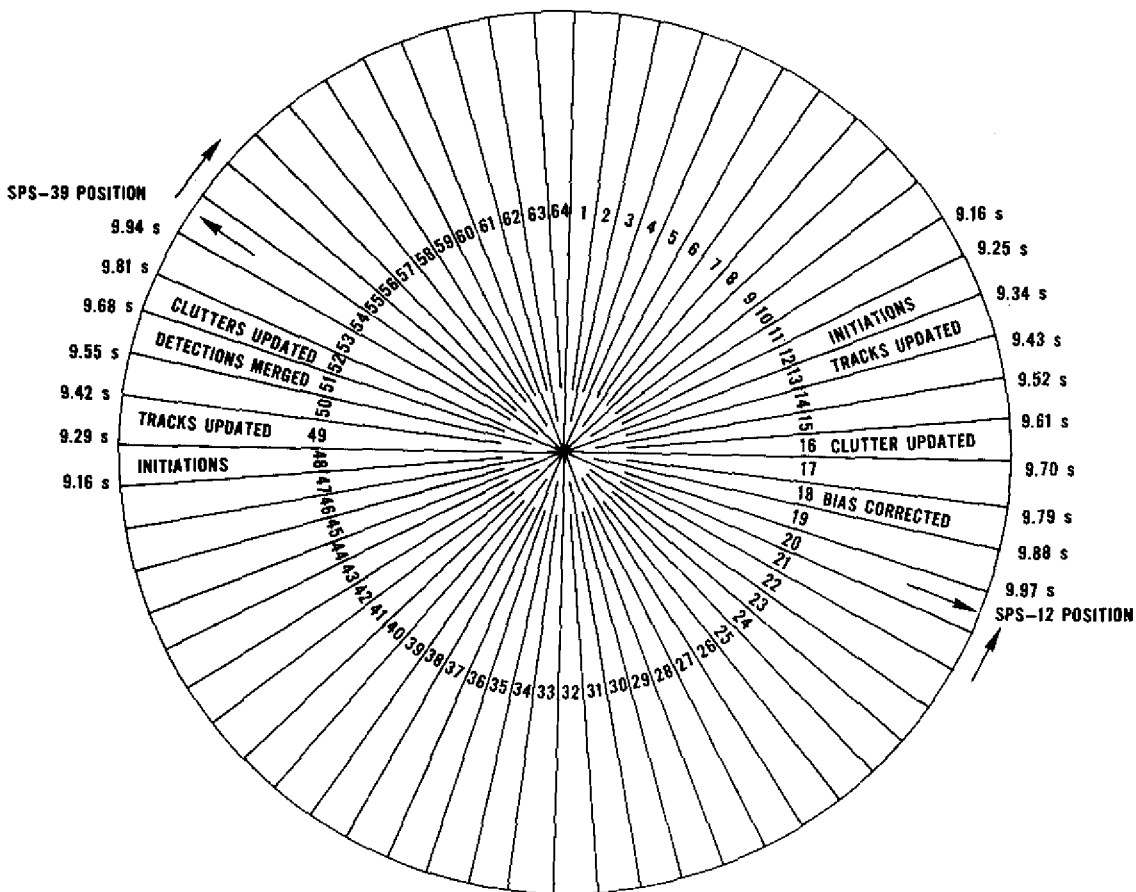


Fig. 16 — Sectoring operation where, for ease of viewing, the scan time of the SPS-12 is 5.76 s, and the Scan Time of the SPS-39 is 8.32 (Present time is 10 s)

four sectors so that the detections update the nearest track. This approximation to the maximum likelihood correlation technique is described in Ref. 4. In this example, tracks in sector 49 are correlated with detections in sectors 48, 49, 50, and 51. Finally, tracks and clutter points are initiated in the sector behind the sector where tracks are updated. In this example, sector 48 is the initiation sector. A detection that is unused and has not updated a track or fallen in a clutter correlation region is used to initialize both a track and a clutter point. The basic idea is that because the clutter correlation regions is very small, a detection from a moving target will not be associated with the clutter point and will be available to update the target. The clutter point, not being updated, will soon be dropped. The method provides extremely rapid track initiation, but has the tendency to generate false tracks.

Updating with the SPS-12 is quite similar to updating with the SPS-39. The major differences are that (a) there is no necessity to merge detections of the SPS-12 (this has been done in hardware), (b) there is an azimuth bias correction applied to the SPS-12 five sectors in advance of the track sector (the bias correction is discussed fully in a forthcoming section), and

(c) there are also various minor differences [2,4], such as declaring a clutter point to be a slowly moving target, etc.

Referring to Fig. 16, the tracking sectors will be processed in the following order: 12 (SPS-12), 49 (SPS-39), 13 (SPS-12), 14 (SPS-12), 50 (SPS-39), 15 (SPS-12), 51 (SPS-39), 16 (SPS-12), 17 (SPS-12), 52 (SPS-39), 18 (SPS-12), 53 (SPS-39), 19 (SPS-12), etc. Obviously, the average processing time must be smaller than the rotation time, or else the processing would lag further and further in time. Consequently, because processing time is usually smaller than rotation time, the system is restricted to operate at least five SPS-12 sectors and six SPS-39 sectors behind their respective radars. When the system is all caught up (i.e., the next sector to be processed has too small a lag), it either works on operator requests or waits until processing can be performed.

Next, the modifications made to the tracking system that have not been documented will be discussed.

### Dual Clutter Map

In the original tracking system [2], there was only one clutter map, no distinction being made whether the clutter point was being updated by the SPS-12 radar, the SPS-39 radar, or both. However, preliminary investigation revealed that clutter points were basically being updated by either one or the other radar, not both. Consequently, if there were two distinct clutter maps, it would be possible to track a target with the SPS-12 over SPS-39 clutter, or vice versa. The parameters associated with the clutter files are as follows:

NC	Clutter number
FULLC	Number of available clutter numbers
NEXTC	Next clutter number available
LASTC	Last clutter number not being used
LISTC(256)	File whose 256 locations correspond to clutter numbers
RPC(NC)	Range of clutter point
APC(NC)	Azimuth of clutter point
ITC(NC)	Last time appropriate radar updated the clutter
RC(NC)	Range of point clutter stored every eight scans of the SPS-39
CBX12(I)	First SPS-12 clutter number in sector I (a subscript of array IDC)
CBX39(I)	First SPS-39 clutter number in sector I (a subscript of array IDC)
IDC(256)	File corresponding to the 256 clutter numbers and containing the next clutter number in a sector or a 0 indicating that this is the last clutter in a sector

The clutter points are updated by correlating only the SPS-12 and SPS-39 detections with clutter points in their respective clutter maps. The clutter numbers associated with the SPS-12

radar in sector I are CBX12(I), IDC(CBX12(I)), IDC(IDC(CBX12(I))), . . . , and those associated with the SPS-39 are CBX39(I), IDC(CBX39(I)), IDC(IDC(CBX39(I))), . . . , with the sequences ending when a zero is obtained. In the initiation sector (sector 48 in the previous examples), an unused detection (did not update a track or lie in a clutter correlation region) is used to initiate a track and a clutter point in *each* clutter map. A clutter point must be generated in each clutter map because if the detection were a clutter detected by both radars, and if a clutter point were not generated in the noninitiating clutter map, the detection from the noninitiating radar would not correlate with a clutter point and would update the initiated track, eventually establishing a firm track. On the other hand, if the detection were a clutter detected by only one radar, the clutter point in the noninitiating clutter map would never be updated and would be dropped after a time TCMAX. Preliminary results on the operation of the dual clutter map can be found in a later section.

### Tracking Filter

In a previous report [4], an adaptive  $\alpha$ - $\beta$  filter was described. This filter was used for over a year and produced accurate tracks. A typical track is shown in Fig. 17. The triangles represent detections of the SPS-12, the circles represent detections of the SPS-39, and the straight line is the predicted position of the target generated by the adaptive filter. Although many detection opportunities are missed, a very accurate track is obtained.

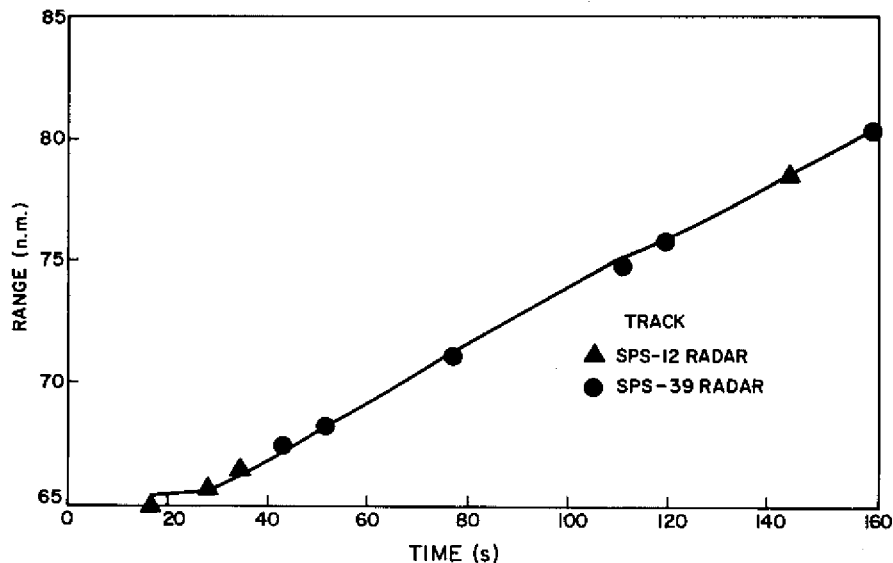


Fig. 17 — Typical track from the ADIT system using an adaptive  $\alpha$ - $\beta$  filter.  
(Typical error is less than 300 m (1000 ft).)

Unfortunately, the adaptive filter requires the storage of six additional arrays beyond the normal requirements of the  $\alpha$ - $\beta$  filter. Because the program is written in Fortran and the NOVA 800 Fortran compiler is very inefficient, which resulted in all available core (32 000) locations being used, a new  $\alpha$ - $\beta$  filter was implemented. The filter, which is a decreasing bandwidth filter with a turn detector, is described in the next paragraph.

The  $\alpha$ - $\beta$  filter equations used after a firm target has been established are

$$x_s(k) = x_p(k) + \alpha_k [x_m(k) - x_p(k)], \quad (3)$$

$$v_s(k) = v_s(k-1) + \left\{ \frac{\beta_k}{T_k} \right\} [x_m(k) - x_p(k)], \quad (4)$$

$$x_p(k+1) = x_s(k) + v_s(k) T_{k+1} \quad (5)$$

where

$x_s(k)$  = smoothed position,

$x_p(k)$  = predicted position,

$\alpha_k, \beta_k$  = system gains,

$v_s(k)$  = smoothed velocity,

$T_k, T_{k+1}$  = sampling periods,

$x_m(k)$  = measured position.

The system gains,  $\alpha_k$  and  $\beta_k$ , are set by

$$\alpha_k = 1 - \exp(-2\xi\omega_0 T_k) \quad (6)$$

$$\beta_k = \frac{\alpha_k^2}{2 - \alpha_k} \quad (7)$$

where  $\xi$  is the filter damping coefficient (set to 0.6) and  $\omega_0$  is the filter bandwidth. The filter bandwidth is calculated from

$$\omega_0 = \frac{\text{IFLTN}}{\text{IFLTD} + \text{MANT}} \quad (8)$$

where IFLT<sub>N</sub> and IFLT<sub>D</sub> are filter parameters whose present values are 375 and 2250, respectively, and MANT is the time interval in counts during which an accurate track is being maintained. (In the computer, 125 counts is 1 s.) When a track is made firm, MANT is set to 2500. When a track is updated with a small range error, MANT is set by the expression

$$\text{MANT} = \text{MIN}\{\text{MANT} + T_k, 11\ 250\}, \quad (9)$$

and when a track is updated with a large range error (indicating a maneuver), MANT is set back to 11 (an arbitrary small number for debugging purposes). Specifically, a range error is small or large depending on whether the absolute difference between the predicted and measured range,  $|RPT(1) - RM|$ , is less than IRCRIT, normally 45 counts ( $\approx 850$  m). Thus,  $\omega_0$  falls to 1/36 for an accurate track and rises to 1/6 when a large error is encountered. (One should also bifurcate the track when a large error is encountered.) However,  $\omega_0$  may presently be too low for tracks that are slowly turning; i.e., the error slowly builds up until the bandwidth is increased. Consequently, new values of IFLT<sub>N</sub> = 500, IFLT<sub>D</sub> = 3000, and Max {MANT} = 9500 are being tested. These correspond to a minimum value of 1/25 and a maximum value of 1/6 for  $\omega_0$ .

Tentative tracks are updated in a different manner. First, for a tentative track the smoothed position is always set equal to the latest measurement; i.e.,  $RS(NT) = RM$  and  $AS(NT) = AM$ . At initiation time  $MANT$  is set to zero; and thus,  $MANT$  is the time since initiation. If  $MANT$  is less than 250 (2 s), the velocities are kept at zero. However, if  $MANT$  is greater than 250, the velocities are calculated by dividing the difference between the measurement and original position by the time difference; i.e.,

$$VRS(NT) = \frac{RM - NR(NT)}{MANT(NT) * 31\ 250} \quad (10)$$

where  $VRS(NT)$  is the smoothed range velocity for target number  $NT$ ,  $RM$  is the range measurement,  $NR(NT)$  is the initiation range, and 31 250 is the appropriate conversion factor.

If a tentative track is not updated within every  $TNMAX$  counts (presently 2100), the tentative track is dropped. If a tentative track is updated after  $TFIX$  counts (presently 2300), a track is made firm. Since currently  $TFIX$  is greater than  $TNMAX$ , at least three detections are required to change a tentative track to a firm track. This logic, along with the new correlation logic, is intended to reduce the number of false tracks.

### Correlation Logic

In a recent report [4], a series of correlation regions was used to approximate the maximum likelihood method of correlation in which the detection is associated with the closest track. This basic technique will be illustrated with the example shown in Fig. 17. There are presently five track correlation regions whose values are

$CRT(5) = 32$	$CAT(5) = 128$
$CRT(4) = 64$	$CAT(4) = 216$
$CRT(3) = 96$	$CAT(3) = 256$
$CRT(2) = 144$	$CAT(2) = 320$
$CRT(1) = 192$	$CAT(1) = 384$

where  $CRT(\cdot)$  is the range value and  $CAT(\cdot)$  is the azimuth value. The correlation logic contains the following steps:

1. First, all the detections falling within the smallest correlation region centered at the predicted position of the first track in the principal tracking sector (sector 49 in example) are identified. Note, detections in sectors 48, 49, 50, and 51 are always used for updating the principal sector. If there are any detections in the correlation region, the *closest* one in the *maximum likelihood sense* [4] is found. Then, this track and detection are said to be associated and are eliminated from future consideration. Other detections, which were in the correlation region, are free to update other tracks.

2. The smallest correlation region is then used with the next track in the principal tracking sector. Again, if no detections are in the correlation region, nothing happens, and if there are detections in the correlation region, the closest pair is associated and eliminated from further consideration.

3. After all the tracks in the principal tracking sector have been used, the smallest correlation region is used with the tracks in the next sector. Specifically, tracks in sector 50 are correlated with detections in sectors 49, 50, and 51 using the previous logic, and the detection closest to the track (within the correlation region) is flagged. This inhibits updating a track in sector 49 with a detection that should update a track in sector 50.

4. Finally, tracks in sector 51 are correlated with detections in sectors 50 and 51. Next, the whole procedure is repeated using the second smallest correlation region. The tracking program discussed in NRL Report 7952 [4] repeated the procedure until all five correlation regions were used. At this time, all flags were removed.

The new tracking program differs from the previous program by making the number of correlation regions used a function of the track quality. Specifically,

Five regions: default option, program reverts to old method (NKON = -5)

Four regions:

(a) Tentative track with  $MANT \leq INIT$  (presently set to 700)

(b) Firm track with time since last update  $\geq 2500$  and  $MANT \leq 1250$

Three regions:

(a) Firm track with time since last update  $\geq 2500$

(b) Firm track with  $MANT \leq 1250$

Two regions:

(a) Tentative track with  $MANT > INIT$

(b) Firm track.

A track uses the largest number of correlation regions for which it qualifies.

#### Radar Bias Correction

If the two radars are not aligned in azimuth, a track similar to the one shown in Fig. 18 results. In this example, the azimuth differences is about a degree, with the SPS-39 reporting a smaller azimuth than the SPS-12. While it is difficult to set both radars to the true azimuth, it is relatively easy to align the radars using the track data.

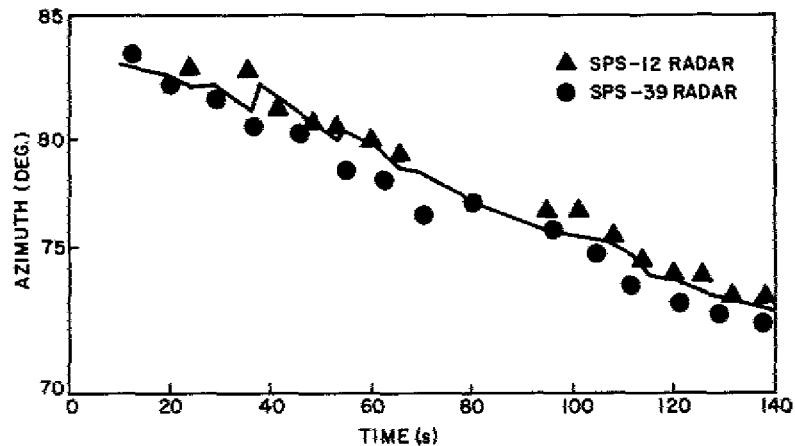


Fig. 18 — Track from the ADIT system illustrating the effects of non-alignment of the azimuth of the SPS-12 and SPS-39 radar

Specifically, it is assumed that the SPS-39 is the correct radar, and the SPS-12 data is then adjusted to obtain the same azimuths. The bias correction (JBIAS) is made by accumulating NEA (presently 10) differences between the predicted azimuth and measured azimuth on the SPS-12 radar. Only tracks that are beyond 4000 range counts ( $\approx 40$  n.mi.) and have been updated by the SPS-39 in the last 1250 time counts (10 s) are considered. After NEA differences are accumulated in JBS a new bias correction is obtained by calculating

$$JBIAS = JBIAS + \frac{JBS}{IFC} \quad (11)$$

where the weighting  $IFC = 100$ .

Of course, if there is a large azimuth differences between the two radars, no tracks will be carried on both radars and no bias correction can be made. Since the largest azimuth correlation region for good tracks is 216 azimuth counts, the radars should be aligned within  $2^\circ$  to obtain convergence. The problems of the size of the azimuth difference that can be corrected and the rate of convergence are mentioned briefly in a later section.

### Input Structure

Since the most effective value of many of the parameters is unknown, a flexible input structure has been developed to facilitate parameter modification for experimentation. At the beginning of each run, the computers request changes by printing

ALTERATION: INDEX AND NEW VALUE.

If no changes are to be made, 0,0 is entered and the default values are used. A list of the parameters that can be changed and their default values are given in Table 1. A change is made by entering the index of the parameter and the new value. For instance, the entry 11, 17 would cause the range of the clutter correlation region for the SPS-12 to be increased from 9 to 17 counts. Furthermore, a parameter may be changed during operation by using option 6 on the alphanumeric display.

### Output Structure

Because the 32 767 storage locations are almost all used, an analysis of the tracking data could not be incorporated into the program. Consequently, provision has been made for printing out the program storage arrays. After stopping and restarting the program, the computer requests instructions by printing

PRINT CONTROL: NONE (1), HANDOFF (2), SELECTIVE (3).

Entering a "1" indicates no output is desired, in which case the program next asks for the alterations discussed in the previous section.

Entering a "2" indicates that the parameters associated with a target being handed off are to be printed out. A typical printout is shown in Fig. 19a. The eight variables printed are as follows:

- The radar with the opportunity to detect the target
- Measured range in nautical miles (0 indicates target not detected)

Table 1 — Input Parameters and Their Default Values

Parameter Index	Parameter Designation	Default Value	Function of Parameter
1	IREAL	0	Type of data: 0 (real) or 1 (simulated)
2	IBIAS	64	1/4 of elscan bias
3	NSEL	2	Number of scans between elscans
4	IBIAT	125	Prediction bias for handoff
5	IBIAS	Previous Value	Bias between radars
6	IFC	100	Weight factor in bias correction
7	NEA	10	Number of terms accumulated for bias correction
8	IRTEN	4096	Range beyond which clutter points are not established
9	MAXR	49	Range change for moving clutter point to track file
10	MINR	49	Range change for moving track to clutter file
11	CRC12	9	Clutter correlation region: range for SPS-12
12	CAC12	128	Clutter correlation region: azimuth for SPS-12
13	CRC39	17	Clutter correlation region: range for SPS-39
14	CAC39	128	Clutter correlation region: azimuth for SPS-39
15	VAMIN	400	Minimum azimuth velocity for a nonchanging range track
16	TNMAX	2100	Time to retain tentative track
17	TFIX	2300	Time necessary for declaring track firm
18	TTMAX	5000	Time to retain firm track
19	TCMAX	4125	Time to retain clutter point
20	NKON	4	Number of correlation regions considered
21	IRCRIT	45	Critical range for track bandwidth change
22	IFLTN	375	Numerator of filter bandwidth
23	IFLTD	2250	Denominator of filter bandwidth
24	INIT	700	Time beyond which tentative track uses two correlation regions
25	IMANT	2500	Initial value of MANT for firm tracks
26	IRNER	1024	Minimum range for establishing tracks
27	IR39U	2048	Blanking range for upper beam of SPS-39

Table 1 (Continued) -- Input Parameters and Their Default Values

Parameter Index	Parameter Designation	Default Value	Function of Parameter
28	CRT(1)	192	5th smallest range correlation region
29	CRT(2)	144	4th smallest range correlation region
30	CRT(3)	96	3rd smallest range correlation region
31	CRT(4)	64	2nd smallest range correlation region
32	CRT(5)	32	Smallest range correlation region
33	CAT(1)	384	5th smallest azimuth correlation region
34	CAT(2)	320	4th smallest azimuth correlation region
35	CAT(3)	256	3rd smallest azimuth correlation region
36	CAT(4)	216	2nd smallest azimuth correlation region
37	CAT(5)	128	Smallest azimuth correlation region
38	KCRT(1)	2	
39	KCRT(2)	2	
40	KCRT(3)	2	
41	KCRT(4)	2	
42	KCRT(5)	2	Compensation values for
43	KCAT(1)	4	maximum likelihood correlation
44	KCAT(2)	4	
45	KCAT(3)	4	
46	KCAT(4)	5	
47	KCAT(5)	5	
48	LAGMX	50	Maximum lag on SPS-12 for skipping sectors
49	IOUT	10	Code number for output device: 10 is Teletype, 12 is line printer
50	MNTMX	11250	Maximum value of MANT

- Predicted range in nautical miles
- Measured azimuth in degrees
- Predicted azimuth in degrees
- Internal clock in seconds (clock cycles every 32768/125 s)
- Range velocity in knots
- Heading in degrees

In the latest version of the program, the track quality parameter MANT is printed instead of the heading, nondetections are not printed out, and the track number is printed alongside the radar, see Fig. 19b.

Entering a "3" indicates that selective variables are to be printed, and the program responds by printing:

ARRAY NUMBER AND START AND END OF ARRAY.

TRUNK, WILSON, CANTRELL, ALTER, AND QUEEN

RADAR	RM	RP	AM	AP	TIME	R VEL.	HEADING
2	33.14	32.95	261.0	261.3	216.415	81.56	171.
9	33.14	33.04	260.6	261.0	219.767	81.56	171.
2	0.00	33.11	0.0	260.7	222.743	81.56	170.
9	33.47	33.18	259.1	260.1	227.887	81.56	170.
2	0.00	33.27	0.0	259.7	229.167	86.00	169.
2	0.00	33.37	0.0	258.8	235.591	86.00	168.
9	0.00	33.38	0.0	258.7	235.999	86.00	168.
2	0.00	33.48	0.0	257.9	241.919	86.00	167.
9	0.00	33.52	0.0	257.6	244.231	86.00	167.
2	0.00	33.58	0.0	257.0	248.335	86.00	167.
9	0.00	33.65	0.0	256.4	252.479	86.00	166.
2	34.37	33.68	255.3	256.2	254.871	86.00	166.
9	0.00	34.30	0.0	254.9	260.727	113.38	164.
2	0.00	34.28	0.0	254.8	261.215	113.38	164.
2	0.00	34.44	0.0	254.0	5.511	113.38	164.
9	0.00	34.48	0.0	253.7	6.823	113.38	163.
2	0.00	34.62	0.0	253.1	11.951	113.38	163.
9	35.27	34.71	252.2	252.6	15.071	113.38	162.
2	35.52	35.13	252.0	252.0	18.399	133.22	162.
9	0.00	35.34	0.0	251.4	23.191	133.22	161.
2	35.93	35.37	250.7	251.2	24.847	133.22	161.
2	0.00	35.70	0.0	250.4	31.191	138.84	160.
9	0.00	35.69	0.0	250.2	31.431	138.84	160.
2	0.00	35.87	0.0	249.4	37.623	138.84	159.
9	0.00	35.95	0.0	249.1	39.679	138.84	159.
2	37.00	36.08	247.9	248.5	44.159	138.84	158.
9	0.00	37.25	0.0	247.4	47.919	295.90	202.
2	0.00	37.39	0.0	246.9	50.399	295.90	201.
9	37.91	37.79	246.2	246.0	56.167	295.90	201.
2	37.82	37.90	246.2	246.2	56.943	311.29	201.
2	0.00	38.39	0.0	245.4	63.279	311.29	200.
9	38.40	38.44	245.2	245.0	64.415	311.29	200.
2	38.65	38.82	244.7	244.5	69.815	311.29	199.
9	38.89	38.98	244.4	244.2	72.655	304.48	199.
2	39.14	39.22	243.8	243.8	76.255	304.48	198.
9	0.00	39.57	0.0	243.3	80.775	304.48	198.
2	0.00	39.62	0.0	242.9	82.583	304.48	197.
2	0.00	40.04	0.0	241.8	89.023	304.48	196.
9	40.04	40.06	242.1	241.8	89.023	304.48	196.
2	0.00	40.55	0.0	241.2	95.351	304.48	196.
9	40.70	40.61	241.6	240.6	97.263	304.48	195.
2	0.00	40.98	0.0	240.5	101.799	304.48	195.
9	41.20	41.20	240.0	239.9	105.519	304.48	194.
2	0.00	41.38	0.0	239.6	108.263	304.48	194.
9	41.69	41.75	239.5	238.8	113.775	304.48	193.
2	0.00	41.77	0.0	239.0	114.711	304.48	194.
2	0.00	42.19	0.0	238.1	121.151	304.48	193.
9	0.00	42.29	0.0	237.9	121.903	304.48	192.

(a) Old printout.

Fig. 19 — Printout associated with a target being handed off.

RADAR	RM	RP	AM	AP	TIME	R VEL.	MANT
2053	13.98	14.49	24.2	22.9	79.575	-1.92	11
2053	13.98	14.00	24.0	24.1	98.783	-0.59	2412
2053	13.98	13.99	24.3	24.0	111.767	-1.48	4035
2040	23.43	23.35	72.9	72.7	151.207	111.16	2947
9040	23.60	23.71	71.2	72.0	164.255	102.23	4578
2040	23.60	23.79	71.7	71.1	170.527	93.84	5362
9040	23.43	23.78	70.5	71.2	172.567	88.81	5617
9040	23.27	23.92	70.2	70.4	180.903	-88.07	11
9040	22.94	23.20	70.2	69.3	189.215	-134.85	1050
2040	22.45	22.59	69.4	69.2	202.719	-152.17	2738
9040	22.23	22.36	69.5	69.2	205.735	-155.72	3115
9040	21.95	22.03	69.3	68.8	214.055	-161.34	4155
9040	21.29	21.39	68.9	68.6	230.687	-167.26	6234
2040	20.88	20.96	69.1	68.5	241.407	-170.08	7574
2040	20.06	20.23	68.0	68.2	260.695	-176.59	9985
9031	25.57	25.39	47.0	45.8	134.311	.19	4592
9031	25.57	25.38	46.7	47.1	142.607	-69.72	5629
9031	25.57	25.32	47.1	47.1	150.919	-59.80	6668
9031	25.57	25.24	47.1	47.5	167.503	-45.14	8741
9031	25.41	25.33	47.1	47.5	175.807	-43.66	9779
9031	25.57	25.31	47.2	47.6	184.111	-38.78	10817
9031	25.57	25.33	46.9	47.7	192.295	-34.19	11250
9031	25.57	25.35	47.1	47.7	200.735	-30.04	11250
9095	24.25	24.35	84.5	84.6	234.735	63.35	4576
9095	24.42	24.37	85.1	85.0	243.031	65.72	5613
9095	24.75	24.66	86.0	85.9	259.655	70.46	7691
2095	24.75	24.75	86.6	86.0	0.775	70.46	8098
2095	24.91	24.84	86.3	86.4	7.207	71.94	8902
2095	25.00	24.94	87.1	86.7	13.647	72.97	9707
9095	25.08	25.09	87.6	87.2	22.503	72.82	10814
9095	25.24	25.22	88.1	87.8	30.815	73.12	11250
9095	25.24	25.34	88.4	88.3	39.127	71.20	11250

(b) New printout.

Fig. 19 (Continued) — Printout associated with a target being handed off.

The basic contents of the eight arrays are as follows:

Array No. 1	SPS-12 detection data
Array No. 2	SPS-39 detection data
Array No. 3	SPS-12 sector data
Array No. 4	SPS-39 sector data
Array No. 5	Clutter files
Array No. 6	Clutter parameters
Array No. 7	Track files
Array No. 8	Track parameters

The specific variables of the eight arrays are given in Table 2. Thus, an entry of "8, 1549, 1676" causes the last times the tracks were updated to be printed out.

Table 2 — Specific Output Variable

Array Number	First Location	Last Location	Contents
1	1	256	RM12: range measurement from SPS-12
	257	512	AM12: azimuth measurement from SPS-12
	513	768	TM12: time measurement from SPS-12
2	1	256	RM39: range measurement from SPS-39
	257	512	AM39: azimuth measurement from SPS-39
	513	768	TM39: time measurement from SPS-39
	769	1024	EM39: elevation measurement from SPS-39
3	1	64	MRK12: time SPS-12 crosses sector
	65	128	NP12: position pointer to last detection in sector
	129	192	NB12: number of detections in sector
	193	256	P1239: position of SPS-39 when SPS-12 crosses sector boundary
	257	257	I12T: last sector SPS-12 crossed
	258	258	I12D: sector in which tracks are presently being updated by SPS-12
4	1	64	MRK39: time SPS-39 crosses sector
	65	128	NP39: position pointer to last detection in sector
	129	192	NB39: number of detections in sector
	193	256	P3912: position of SPS-12 when SPS-39 crosses sector boundary
	257	257	I39T: last sector SPS-39 crossed
	258	258	I39D: sector in which tracks are presently being updated by SPS-39
5	1	64	CBX12: first SPS-12 clutter point in sector
	65	128	CBX39: first SPS-39 clutter point in sector
	129	384	IDC: contains next clutter number in sector or a zero indicating last track number

Table 2 (Continued) — Specific Output Variable

Array Number	First Location	Last Location	Contents
6	385	640	LISTC: file of available clutter numbers
	641	641	NEXTC: next clutter number available
	642	642	LASTC: last clutter number not being used
	643	643	FULLC: number of available clutter numbers
	644	644	I12DEL: SPS-12 processing lag (I12T-I12D)
	1	256	RPC: range of clutter point
	257	512	APC: azimuth of clutter point
7	513	768	ITC: last time appropriate radar updated the clutter
	769	1024	RC: range of clutter, stored every 8 scans of SPS-39
	1	64	TBX: first track number in sector
	65	192	IDT: contains next track number in sector or a zero indicating last track number
8	193	320	LISTT: list of available track numbers
	321	321	NEXTT: next track number available
	322	322	LASTT: last track number available
	323	323	FULLT: number of available track numbers
	324	324	I39DEL: SPS-39 processing lag (I39T-I39D)
	1	128	RPT: predicted range of track
	129	256	APT: predicted azimuth of track
	257	384	ES: smoothed elevation of track
	385	512	VRS: range velocity of track
	513	640	OUT: output parameters for alphameric display
	641	652	ISTA: status parameters
	653	780	RS: smoothed range of track
	781	908	AS: smoothed azimuth of track
	909	1036	VAS: azimuth velocity of track
	1037	1164	TT12: last time SPS-12 updated the track
1165	1292	TT39: last time SPS-39 updated the track	
1293	1420	TTL12: next time SPS-12 will pass over target	
1421	1548	TTL39: next time SPS-39 will pass over target	
1549	1676	TT: last time track was updated	
1677	1804	KT: initial azimuth position for tentative tracks and initial detection time for firm tracks	
1805	1932	TF: minus initial detection time for tentative tracks and elevation scan parameter for firm tracks	
1933	2060	MANT: time small-filter bandwidth has been used	
2061	2188	NR: smooth range stored every 8 scans of SPS-39	
2189	2189	NTARGET: number of firm tracks	
2190	2190	NELEV: number of targets in elevation scan	
2191	2191	ISKIP: number of times sectors skipped	

### Alphanumeric Display

The alphanumeric display is shown in Fig. 20. The radar operator requests data by entering three parameters: an operator code (IOPER) from the 10 buttons in the upper right-hand corner and two modifying parameters (IPAR1 and IPAR2) from the 10 buttons in the middle right-hand portion of display. These three parameters are entered via a DMA channel into the computer. After the request has been processed, IOPER is set to -1, and NUM is set equal to the number of tracks that fulfill the request. Since the pertinent track parameters (RPT, APT, ES, and OUT) are accessed every second via a DMA, only the track numbers fulfilling a request, JTAR (1) to JTAR (NUM), must be supplied.

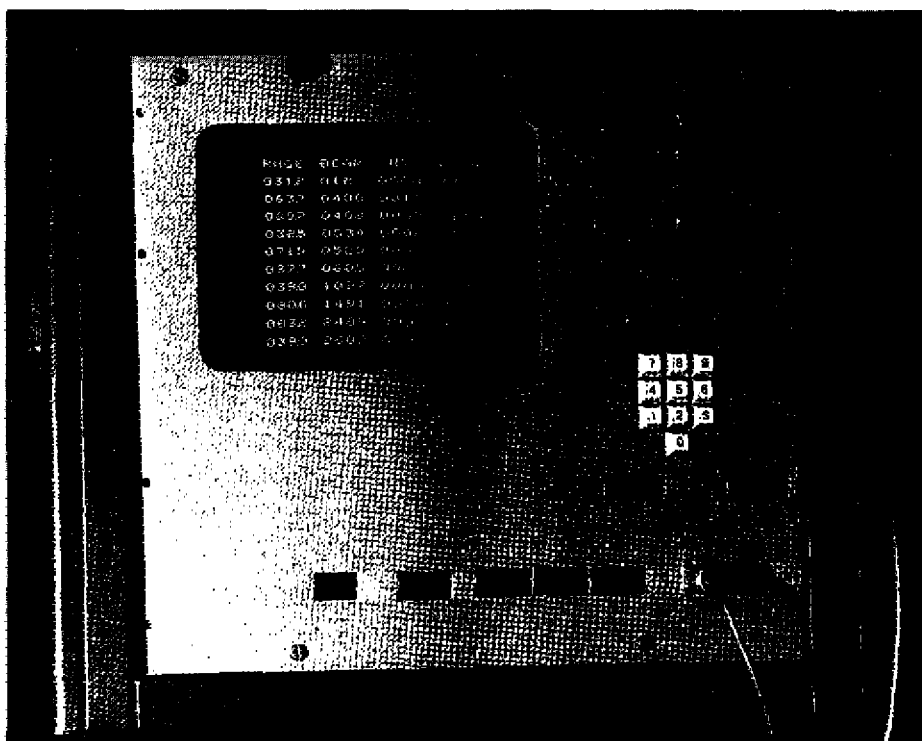


Fig. 20 — Photograph of alphanumeric display

The operator requests and their appropriate parameters are given in the following list:

- IOPER = 1 Track handoff
  - IPAR1 = track number
  - IPAR2 = 1 End handoff request
- IOPER = 2 List tracks within an azimuth interval
  - IPAR1 = first azimuth (deg)
  - IPAR2 = second azimuth (deg)
- IOPER = 3 List tracks inside or outside a designated range

IOPER =

IPAR1 = range (n.mi.)

( )

- IOPER = 4 List tracks with MANT's greater than  $100 \times \text{IPAR1}$   
 IPAR1 = designated MANT/100 (counts)
- IOPER = 5 List firm tracks
- IOPER = 6 Dual function  
 IPAR1 = 0 List tentative tracks  
 IPAR1  $\neq$  0 Change input parameter. Specifically, the 2 most significant digits of IPAR1 are the parameter to be changed, and 1000 times the last digit of IPAR1 plus IPAR2 is the new value. JTAR (1) returns with 240, indicating that the change has been made.
- IOPER = 7 List high-closing-velocity tracks  
 IPAR1 = Velocity (knots)
- IOPER = 8 List tracks under elevation search
- IOPER = 9 Request for elevation on track  
 IPAR1 = track number  
 IPAR2 = 1 End elevation request
- IOPER = 10 Enter noninitiating sectors  
 IPAR1 = initial range or azimuth  
 IPAR2 = final range or azimuth

A noninitiating sector, inhibiting initiation of clutter points and tracks, is entered by first entering the range boundaries. After a 200 is returned in JTAR(1), the azimuth boundaries are entered. The second operator request can be a 2 (sector is only for SPS-12), a 9 (sector is only for SPS-39), or a 10 (sector is for both radars). A  $200 + N$  in JTAR signifies that the  $N$ th sector has been entered. Four sectors can be entered and any additional sectors replace the fourth sector. All the sectors can be removed by letting IPAR1 = IPAR2. As an example, the entry

10, 30, 60  
 2, 10, 25

causes the inhibiting of tracks and clutter points for the SPS-12 radar in a sector running from 30 to 60 n.mi. and from  $10^\circ$  to  $25^\circ$ . However, as indicated later, only track initiation should be inhibited.

### Status Parameters

The first 11 status parameters are displayed by using an 11-position switch on the alphanumeric display. The parameters are as follows:

- ISTA(1) = number of firm tracks
- ISTA(2) = number of firm plus number of tentative tracks
- ISTA(3) = number of clutter points
- ISTA(4) = time for SPS-12 to accumulate 256 detections (s)
- ISTA(5) = processing lag on SPS-12 (I12DEL)
- ISTA(6) = time for SPS-39 to accumulate 256 detections (s)
- ISTA(7) = number of detections stored in handoff routine
- ISTA(8) = bias in counts between SPS-12 and SPS-39

- ISTA(9) = number of clutter points transferred to the track file every eighth scan of SPS-39  
 ISTA(10) = number of tracks transferred to the clutter file every eighth scan of the SPS-39  
 ISTA(11) = number of inhibiting sectors  
 ISTA(12) = 1 indicates that sectors have been skipped during last scan of SPS-39 (ISKIP)

Because only one parameter can be viewed at an instant and because it is very important to know if sectors are being skipped, a light is turned on when ISTA(12) has a nonzero value.

## TRACKING RESULTS

So far, only a preliminary data analysis has been performed. However, tracking results will be presented to indicate system performance and illustrate problem areas. Several of the experiments were run before all the changes in the previous sections were made. They have been included because they dictated several of the changes. Experiments 1, 2, and 3 were run on May 18, 1976, and experiments 4 and 5 were run on September 3, 1976.

### Experiment 1 (SPS-12 Only)

The tracking parameters used in this experiment are the default values listed in Table 1 with the following changes: (16, 3150), (17, 1250), (21, 70), (24, 10 000), (33, 400), (34, 352), (35, 296), (38, 12), (39, 9), (40, 12), (41, 8), (42, 4), (43, 25), (44, 22), (45, 37), (46, 27), and (47, 16). Most of these changes are minor ones affecting the correlation region size and determination of the closest detection to a track. However, the first two changes with parameter 16 greater than parameter 17 means that many times only two detections are required to make a track firm. Also affecting the initiation process is the fact that all correlation regions were used for tentative tracks. This was accomplished by setting parameter 24 to a large value.

In this experiment, the SPS-12 accepted detections only between 0° and 90°, and the SPS-39 was censored completely. A limited area was used so that various files would not be overwritten with new data. This fact aids greatly in interpretation of the data. After operating the tracking system for 11 scans, the system was stopped, and arrays 6 (clutter files) and 8 (track files) were printed out. An analysis of the data was performed, and a history of the uncorrelated detections on a scan-by-scan basis is shown in Table 3.

The first scan was only a partial scan with the tracking system being started at 22°. During this initial scan 22 detections were reported with 2 at far range, greater than IRTEN. Of the 20 clutters initiated, 13 were updated, and 7 were never updated. Ten tracks were made firm; however, seven tracks were never updated thereafter. Similar information can be obtained about scans 2 through 7 from the table entries.

The most important conclusion that can be reached by examining Table 3 is that too many false tracks were generated: 20 out of 29 tracks that were declared firm were never updated. While some of this may be due to fading, many are simply false tracks. This is indicated by most of the short tracks being at close range. (Later results, experiment 5, indicate that approximately 15% of the real tracks that are declared firm are never updated.) Therefore, to

Table 3 — Scan-by-Scan Uncorrelated Detection History for the SPS-12

Scan Number	Number of Uncorrelated Detections	Clutter Points		Tracks		
		Updated	Not Updated	Tentative Updated	Firmed, Not Updated	Firmed, Updated
1	22	13	7	0	7	3
2	28	22	4	5	2	3
3	13	5	5	0	1	2
4	4	2	1	0	0	0
5	6	3	0	1	1	0
6	15	8	6	0	3	0
7	15	5	9	0	6	1

avoid this problem, three detections have been required to declare tracks firm, and the number of correlation regions has been decreased for tentative tracks that have been updated.

### Experiment 2 (SPS-39 Only)

The track parameters were the same as those in experiment 1. In this experiment, the SPS-39 accepted detections between 0° and 90°, and the SPS-12 was censored completely. The system was operated for eight scans, and the scan history of uncorrelated detections is shown in Table 4. Of the 14 tracks declared firm, 5 were never updated after being declared firm. Furthermore, many of the updated firm tracks were at short ranges (less than 15 n.mi.), strongly suggesting the possibility that they are just clutter points.

Table 4 — Scan-by-Scan Uncorrelated Detection History for the SPS-39

Scan Number	Number of Uncorrelated Detections	Clutter Points		Tracks		
		Updated	Not Updated	Tentative Updated	Firmed, Not Updated	Firmed, Updated
1	63	34	21	5	2	8
2	8	4	3	0	0	0
3	4	1	3	1	0	1
4	7	5	1	2	3	0

### Experiment 3 (SPS-12 and SPS-39)

In this case, detections from both radars were accepted in a sector: 0° to 90° and 10 n.mi. to maximum range. The track parameters are the same as those in experiment 1. After operating the system for approximately 55 s, the tracking system was stopped, and the entire contents of the clutter files and the tracks files were printed out.

Analysis of the first 80 uncorrelated detections occurring in the first 40 s yielded the following information:

1. Initiation:
  - a. Eighty tracks were initiated.
  - b. Seventy-two clutter points were initiated inside of IRTEN.
2. Clutter map:
  - a. Twelve points were updated by the SPS-12.
  - b. Twenty-one points were updated by the SPS-39.
  - c. Four points were updated by both radars.
3. Track file:
  - a. Seven tracks were carried on the SPS-12.
  - b. Three tracks were carried on the SPS-39.
  - c. Five tracks were carried on both radars.
  - d. Two firm tracks have been dropped.
  - e. One tentative track is presently carried on SPS-12.
  - f. Six tentative tracks were updated but were dropped.
4. Single detections: 25 points were never updated, either as track or clutter points, after initiation.

Adding up the number of clutter updates (37), track updates (24), and single detections (25), one obtains 86. There is a difference between 86 and 80 because 6 clutter points were also updated as tracks: 3 tentatives were dropped, 2 firm tracks were dropped, and 1 firm track was about to be dropped.

Examining the clutter data shows that only 4 of the 37 clutter points are carried on both radars. This is because detections do not occur in homogeneous clutter, but rather occur in the fringe areas; and these areas are different for the two radars. Consequently, it is worthwhile to use individual clutter maps.

The values of MANT for 17 firm targets, in order of initial detections, are 7406, 4959, 6564, 6577, 2500, 6815, 5605, 2500, 6625, 2500, 5342, 4750, 4757, 4132, 2500, 3316, and 2500. The first three 2500's correspond to tracks that were declared firm but were never updated, and the last two correspond to tracks that were just made firm and have had no opportunity to be updated. Thus, while the number of firm tracks, not updated, is less than in experiments 1 and 2, there are still too many false tracks.

No conclusions should be drawn from the fact that there were fewer false tracks present when both radars were operating. This is probably because when both radars are operating, the first 10 n.mi. were censored. The next several experiments were run to investigate the number of false tracks generated.

#### **Experiment 4 (Poor Initiation)**

The tracking parameters are the default values given in Table 1 except for the changes (16, 3150), (17, 1250), and (24, 10 000). Thus, most tracks are initialized by only two detections, and those tracks initialized by more than two detections used all the correlation regions.

Detections were accepted in a sector:  $0^{\circ}$  to  $90^{\circ}$  and 10 n.mi. to maximum range. Data were collected by handing off a track as soon as a track was made firm. After 10 detections

were collected or the track was dropped, the next target that was made firm was handed off. By examining the correlations made, it is rather easy to decide, for the vast majority of tracks, whether a track is a target, clutter, or a bad track (combination of tracks and clutter points). Some typical tracks are shown in Fig. 19b: track 53 has captured a clutter point, track 40 is a turning target, track 31 is a clutter point, and track 95 is a target. During the operation, the average number of tracks declared firm, inside and outside of 25 n.mi., was 18 and 17, respectively. Consequently, it appears that there are many false tracks.

Examining the data indicates that there were 23 tracks saved inside of 25 n.mi. Fifteen of these were never updated, four were targets, two were clutter points, and two appeared to be false tracks. While some of the 15 tracks that were never updated could be real tracks belonging to targets having low blip-scan ratios, most of them are probably falsely initiated tracks. To obtain an estimate of the number of legitimate tracks never updated after initiation, data further than 40 n.mi. were considered.

Examination of the data beyond 40 n.mi. showed, 24 tracks were initiated. Three of these were never updated, 17 were legitimate tracks, 1 was a clutter point, and 3 were false tracks. Thus, it appears that about 15% of the legitimate targets are dropped immediately after being initiated because of low blip-scan ratios.

To reduce the number of false tracks, it was decided to require three detections for track initiation and to require a smaller correlation region for the third detection. Specifically, it is desired that a track be declared firm if one radar detects the target three times out of four opportunities. The initiation logic is based on two time parameters; TNMAX and TFIX. A tentative track is dropped if TNMAX counts occur between detections, and a tentative track is made firm if a detection occurs TFIX counts after initiation. Thus, by setting  $TFIX > TNMAX$ , one can require at least three detections for initiation (if  $TFIX > 2*TNMAX$ , at least four detections are required for initiation). Since the scan rates of the SPS-12 and SPS-39 are 800 and 1000 counts, respectively,  $TFIX < 3*(800)$  and  $TNMAX > 2*(1000)$ . The first condition is imposed by initiating on the fourth scan of the SPS-12, and the second condition is imposed by not initiating with two out of three detections on the SPS-39. With the constraints  $2000 < TNMAX < TFIX < 2400$ , the values  $TNMAX = 2100$  and  $TFIX = 2300$  were chosen.

#### **Experiment 5 (Improved Initiation)**

The tracking parameters are given in Table 1; i.e., three detections are required for initiation, and a smaller correlation regions is used after the second detection (if time since initiation is greater than 700 counts). Detections were accepted between  $0^\circ$  and  $90^\circ$  and 10 n.mi. to maximum range. Data were collected by handing off tracks, as was done in experiment 4.

Examining the data shows that there were 21 tracks saved inside of 25 n.mi. Three of these were never updated, nine were targets, eight were clutter points, and one was a false track. Outside of 25 n.mi. 34 tracks were saved. Five of these were never updated, 27 were targets, one was a clutter point, and one was a false track. A comparison of these values with those of experiment 4 can be made by examining Table 5. Obviously, fewer false tracks (indicated by the number of tracks never updated) are generated by requiring three detections for initiation.

Table 5 — Comparison of Track Initiation Procedures

Detections Required for Initiation	Range Interval (n.mi.)	Tracks Never Updated	Real Targets	Clutter Points	False Tracks
2	< 25	15	4	2	2
	> 25	3	17	1	3
3	< 25	3	9	8	1
	> 25	5	27	1	1

Examination of Table 5 shows unexpectedly that eight clutter points were found in the track files. This was because a noninitiating sector (21 to 22 n.mi. and 0° to 90°) was generated to inhibit sidelobe detections from the Bay Bridge. Since these detections can be used to update tracks, they readily captured tentative tracks adjacent to the noninitiating region. This problem will be remedied by only inhibiting initiation of tentative tracks in inhibiting sectors; i.e., clutter points will be initiated.

To illustrate what is classified as a false track, consider the track parameters shown in Table 6. While the target is obtaining detections with both radars, there is not significant change in range or azimuth. Furthermore, referral to a map indicates that these detections are from the vicinity of a small island (sandbar) in the Chesapeake Bay.

Table 6 — Parameters of a False Track

Measured Parameters				Filter Parameters		
Radar (SPS-)	Time (s)	Range (n.mi.)	Azimuth (deg)	Range (n.mi.)	Azimuth (deg)	Range Velocity (knots)
39	107.9	11.92	81.2	12.22	79.9	142
39	116.2	11.92	81.2	12.32	79.9	117
39	124.6	11.92	81.2	12.34	79.8	97
12	126.5	12.25	81.7	12.21	80.3	98
39	132.9	11.92	80.9	12.36	80.2	83
12	133.0	12.25	82.0	12.23	80.4	83
12	139.4	12.25	82.1	12.35	80.2	80
39	141.2	12.25	82.7	12.36	80.7	79
12	145.9	12.25	81.8	12.43	80.9	75
39	149.5	12.08	82.2	12.46	81.1	69
12	152.4	12.17	81.6	12.43	81.2	67

### Tracking Accuracy

Ideally, the tracking accuracy should be determined by comparing the track to the true position of the target, which is measured by a precision tracking radar. However, this was not possible. Instead, the track was compared to the position measured by either the SPS-12 or SPS-39 radars. The range and azimuth errors, where errors are defined by differences between measurements and tracks, are shown in Table 7 for data taken on May 18, 1976. The average

Table 7 — Differences Between Measurements and Tracks  
(May 76 Data)

Measurement Number	Track No. 1		Track No. 2		Track No. 3		Track No. 4		Track No. 5	
	Range (n.mi.)	Azimuth (deg)								
1	-0.19*	0.3*	-0.08	0.3	-0.13	0.0	-0.34	-0.5	0.16	-2.6
2	-0.10	0.4	0.02	0.3	-0.07	-0.1	-0.43	-0.2	0.00	0.1
3	-0.29	1.0	0.07	0.1	0.01*	0.7*	-0.05	0.0	0.27	-1.1
4	-0.69*	0.9*	0.00	0.0	-0.01	-0.6	-0.30	-0.2	0.05	0.3
5	-0.56	0.4	-0.04	0.1	-0.16	-0.2	-0.10	-1.0	0.23	0.4
6	-0.39*	0.0*	-0.07	0.4	-0.07*	-0.2*	0.03	-0.6	0.30*	0.5*
7	-0.56*	0.5*	-0.10	-0.1	-0.26	0.1	-0.08	-1.2	0.29	0.7
8	-0.92*†	0.6*†	0.04	-0.3	-0.49	0.1	-0.09	0.0	0.11	0.3
9	-0.12	-0.2	-0.01	-0.2	-0.26	0.1	-0.01	-1.3	0.19	0.5
10	0.08*	0.0*	-0.05	-0.2	-0.14	0.3	-0.06	-0.9	-	-
11	0.04	-0.2	-0.13	-0.3	0.01	0.0	-0.10	-0.8	-	-
12	0.17*	-0.2*	-0.16	-0.3	-	-	-0.23	-1.4	-	-
13	0.09	-0.2	0.09	-0.1	-	-	-0.58	-0.5	-	-
14	0.08*	0.0*	0.00	0.1	-	-	-	-	-	-
15	0.02	-0.3	-	-	-	-	-	-	-	-
16	-0.09	-1.0	-	-	-	-	-	-	-	-
17	0.00	-0.1	-	-	-	-	-	-	-	-
18	0.06	-0.7	-	-	-	-	-	-	-	-

\*SPS-12 measurement.

† Filter bandwidth has been increased

and standard deviation of the 65 range errors for the five tracks are  $-0.09$  and  $0.23$  n.mi., respectively. The average and standard deviation of the azimuth errors are  $-0.12^\circ$  and  $0.60^\circ$ , respectively. Except for track 1, these numbers are associated almost exclusively with SPS-39 tracks. The blip-scan ratios, number of detections divided by detection opportunities, for these tracks are given in Table 8. As is readily seen, the SPS-39 detects the target about 60% of its opportunities, and the SPS-12 only 10% of its opportunities, with most of its detections being made on track 1. However, it should be noted that the next day it was decided the crystal in the SPS-12 receiver had degraded, causing a loss in receiver sensitivity.

The history of track 1 is shown in Fig. 19a. While track 1 has associated with it the largest range errors, examination of the track history reveals that the track probably would not have been carried on the SPS-39: there was only one SPS-39 detection in a 90-s interval. Furthermore, the large error is caused by the target's acceleration in range as can be seen in Fig. 21. At the eighth detection ( $t \approx 94$  s), the range error is greater than IRCRIT, the filter bandwidth is increased, and an accurate track is maintained from that time onward.

To obtain a better estimate of the blip-scan ratio and another estimate of the tracking accuracy, the Sept. 3, 1976, data were analyzed. The first 15 tracks recorded are summarized in Tables 9 and 10: Table 9 shows the range and azimuth errors, and Table 10 shows the blip-scan ratio. It is readily seen that the SPS-12 radar supplied as many detections as the SPS-39. The blip-scan ratio was 39% for the SPS-12 and 49% for the SPS-39.

Table 8 — Blip-Scan Ratio of Tracks

Radar	Track 1	Track 2	Track 3	Track 4	Track 5
SPS-12	8/27	0/27	2/22	0/26	1/11
SPS-39	10/21	14/21	9/16	13/21	8/9

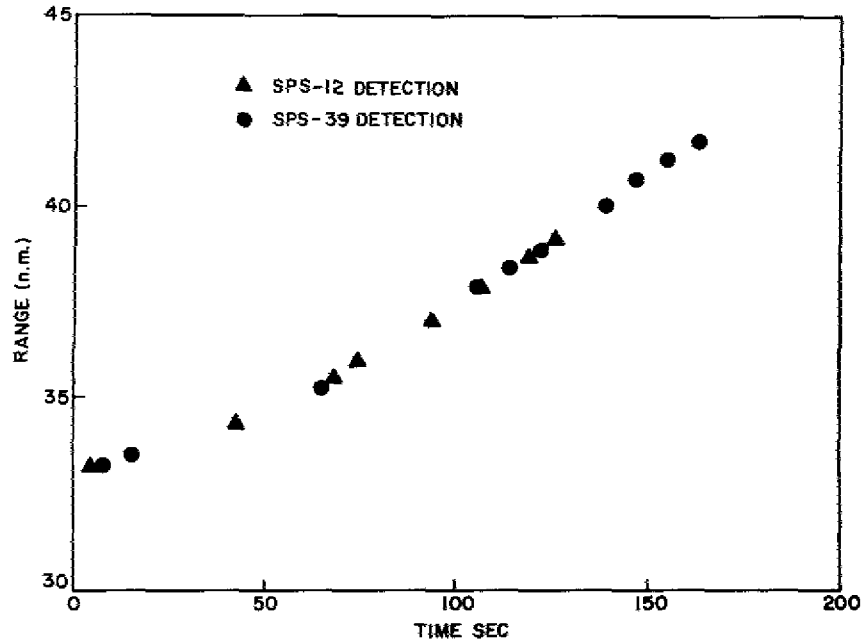


Fig. 21 -- Detection history for track 1 on May 18, 1976

Table 9 -- Differences Between Measurements and Tracks  
(Sept. 76 Data)

Measurement Number	Track No. 1		Track No. 2		Track No. 3		Track No. 4		Track No. 5	
	Range (n.mi.)	Azimuth (deg)								
1	0.08*	0.2*	-0.10	-0.1	-0.13	0.3	-0.04*	-0.1*	-0.13	-1.3
2	-0.11	-0.8	0.05	0.1	-0.19	0.5	0.00	0.3	-0.08*	-0.2*
3	-0.17*	0.6*	0.09	0.1	0.01*	0.7*	0.02*	0.2*	-0.19*	-0.6*
4	-0.35	-0.7	0.00*	0.6*	0.00	0.2	-0.02	0.2	-0.17	0.1
5	-0.65†	-0.2†	0.07*	-0.1*	-0.02*	-0.7*	-0.04	-0.2	-0.06	0.7
6	-0.26	0.9	0.06*	0.4*	-0.06	-0.3	0.13*	-0.2*	0.81*†	2.2*†
7	-0.14*	0.2*	-0.01	0.4	0.04*	-0.2*	-0.12	-0.1	0.29	3.2
8	-0.08	0.3	-0.02	0.3	0.01*	0.1*	-0.10	-1.0	-	-
9	-0.08	0.5	-0.10	0.1	0.05*	0.6*	-0.42	-1.0	-	-
10	-0.10	0.3	-	-	-0.02*	-0.4*	-0.40*	-0.9*	-	-
11	-0.08*	0.6*	-	-	-	-	-0.55†	-1.1†	-	-
12	-0.17*	-0.2*	-	-	-	-	-0.28*	0.0*	-	-
13	-	-	-	-	-	-	0.11*	-0.1*	-	-
14	-	-	-	-	-	-	0.12	0.4	-	-
RMS Error	0.25	0.52	0.07	0.30	0.08	0.45	0.23	0.56	0.34	1.59

\*SPS-12 measurement.

†Filter bandwidth has been increased.

Table 9 – Differences Between Measurements and Tracks  
(Sept. 76 Data) (Continued)

Measurement Number	Track No. 6		Track No. 7		Track No. 8		Track No. 9		Track No. 10	
	Range (n.mi.)	Azimuth (deg)								
1	-0.02	-0.6	-0.26*	-0.5*	-0.01*	0.1*	0.08*	0.0*	0.11	0.0
2	0.12	-0.6	-0.30*	-0.9*	0.02*	0.4*	-0.03	-0.7	0.40	0.5
3	0.05	-0.3	-0.31*	-0.4*	0.05*	0.9*	-0.03	-0.6	0.05	0.0
4	0.01	0.0	-0.23*	-0.4*	0.07*	0.7*	0.06*	-0.6*	0.10	0.9
5	-0.05*	-0.1*	-0.26*	-0.4*	0.04*	0.1*	0.13	.9	0.04*	-0.3*
6	-0.06	0.1	-0.28*	-0.1*	-	-	0.10	-0.2	-0.09	0.7
7	-0.10*	0.2*	-0.29	-1.2	-	-	0.10*	-0.8*	-0.06	0.5
8	-0.13	-0.1	-0.23*	-0.7*	-	-	0.05	-0.6	0.03	-0.6
9	-0.50*	0.3*	-0.26*	0.2*	-	-	0.13*	0.0*	0.24*	0.1*
10	-0.15	0.0	-0.24*	-0.2*	-	-	0.03	-0.3	-	-
11	-0.06*	0.0*	-0.24*	-0.5*	-	-	-	-	-	-
12	-	-	-0.22*	0.2*	-	-	-	-	-	-
RMS Error	0.09	0.30	0.26	0.56	0.04	0.54	0.08	0.56	0.16	0.50

\*SPS-12 measurements.

†Filter bandwidth has been increased.

Table 9 – Differences Between Measurements and Tracks  
(Sept. 76 Data) (Continued)

Measurement Number	Track No. 11		Track No. 12		Track No. 13		Track No. 14		Track No. 15	
	Range (n.mi.)	Azimuth (deg)								
1	0.09	0.1	0.12	-0.2	-0.07	1.0	0.33*	0.1*	-0.03*	0.3*
2	0.12*	0.2*	0.31	-0.6	0.04*	0.6*	0.13*	-0.1*	0.01*	0.7*
3	0.18*	0.0*	0.17*	0.0*	-0.04	0.7	0.14	0.6	0.00*	-0.5*
4	0.14	0.6	0.30*	-1.1*	0.05*	0.4*	0.17	0.6	0.00*	-0.4*
5	0.10*	0.5*	0.10	-0.3	0.05*	0.7*	0.23	0.6	0.09*	-0.6*
6	0.12*	0.2*	0.18*	0.1*	-0.04	0.5	0.25	0.1	0.00	0.1
7	0.0	0.5	0.20	-0.2	-0.04	0.7	0.33	0.0	0.13	0.1*
8	0.24	0.5	0.35*	0.0*	0.05*	1.3*	-	-	0.17*	-0.2*
9	0.17*	0.0*	0.36	0.1	0.47	-0.4	-	-	0.29*	-0.2*
10	0.16*	0.0*	0.30	0.0	-0.13	0.4	-	-	-	-
11	0.12	0.1	-	-	-0.01*	0.6*	-	-	-	-
RMS Error	0.14	0.33	0.25	0.41	0.15	0.71	0.23	0.39	0.12	0.40

\*SPS-12 measurement.

Table 10 — Blip-Scan Ratio of Tracks

Track Number	SPS-12	SPS-39	Flight Path
1	5/18	7/13	Turn
2	3/13	6/10	Straight
3	6/9	4/7	Straight
4	6/14	8/11	Turn
5	3/19	4/14	Bad track
6	4/9	7/7	Straight
7	11/11	1/9	Straight
8	5/5	0/4	Straight
9	4/8	6/7	Straight
10	2/32	7/25	Straight
11	6/12	5/10	Straight
12	4/13	6/10	Straight
13	5/7	6/6	Straight
14	2/9	5/7	Straight
15	8/12	1/10	Straight
Total	74/191	73/150	—

The RMS range error is 0.18 n.mi. and the RMS azimuth error is  $0.48^\circ$ . (It should be noted that track 5 was excluded from the calculation since the last two detections were falsely correlated to the track just as it was about to be dropped.) Comparison of these numbers with the data of May 18, 1976 indicates a slight improvement in tracking accuracy when tracks are being updated with both radars. No judgments should be made on the relative accuracy of radar integration since these numbers include measurement errors and are probably from targets of significantly different cross sections. For a valid comparison, a dedicated target will be used in future experiments.

### Bias Correction

Data were taken on Sept. 10, 1976 to investigate the bias correction procedure. Since only targets beyond 40 n.mi. are presently used for bias correction, the first 35 n.mi. were censored. Furthermore, it should be noted that it was raining, and, consequently, the performance of the S-band SPS-39 was severely degraded. The experiment was conducted by offsetting the SPS-12 radar by a known bias and recording the bias correction as a function of time. The results for a 50-count offset ( $50/91^\circ$ ) are shown in Table 11. As can be seen, the correction process is slow but steady. The convergent rate can be increased by decreasing IFC (input parameter 6); i.e., decreasing IFC from 100 to 50 doubles the convergent rate. Furthermore, since a target is said to be carried on both radars if each radar detects the target only once in  $TTMAX = 5000$  counts, while a track must be updated by both radars in a 1250-count period to be used for bias correction, it is quite likely that only one or two tracks are being used for bias correction.

To investigate the largest azimuth bias that can be corrected, the SPS-12 was offset by 250 counts. At this offset, no tracks were carried by both radars, and consequently, no bias correction took place. At a 200-count offset, one to two tracks were carried on both radars; it took 10

Table 11 — Time History of Bias Correction

Time (min)	Bias (Counts)	Number of Tracks Being Held by Both Radars	Time (min)	Bias (Counts)	Number of Tracks Being Held by Both Radars
0	50	4	18	20	8
1	50	5	19	19	7
2	49	6	20	19	5
3	48	5	21	19	3
4	45	6	22	19	4
5	42	3	23	19	3
6	41	2	24	19	3
7	40	3	25	13	8
8	40	5	26	12	8
9	35	6	27	9	5
10	34	5	28	9	7
11	34	4	29	9	4
12	31	8	30	10	5
13	25	6	31	6	4
14	25	6	32	6	7
15	24	7	33	2	5
16	23	7	34	1	2
17	22	8	35	0	4

to 15 min for a bias correction; and the correction had a value of 10 to 15 counts. Thus, a 2.5° azimuth bias cannot be corrected, but a 2.0° azimuth bias can be corrected.

## SUMMARY

The ADIT system and various portions of it have been described in previous reports [1-4,6]. The present report reviewed the basic system philosophy, described various modifications, and discussed preliminary results quantifying system performance.

The variable parameters of the ATD system have been set, and a merging circuit for reducing target splits has been built. Analysis of recorded data showed that the ATD system works as anticipated — detecting the targets and limiting the false alarms to a manageable number. The MGST processor, a nonparametric detector with adaptive thresholding, performs extremely well. Although the MGST processor is extremely complicated, it could be simplified by use of new technology. However, we currently believe that the detector should have operator controls for changing thresholds in various sectors.

The tracking has been described previously [2,4]. Various changes have been made to improve tracking performance. Specifically, included in the new tracking program are the following items (a) a dual clutter map, (b) a new tracking filter, (c) a new correlation logic based on track quality, (d) an automatic bias correction between radars, (e) a sector censoring capability, and (f) a program control to facilitate input changes and to expand system monitoring facilities.

During the summer of 1976, the system was operated several times. Many of these tests were used to find useful operating values for system parameters, and these values are listed in Table 1. However, several tests were run to check specific operating performance. From these tests, the following conclusions were drawn:

1. A dual clutter map should be used. Only 10% of the clutter points were tracked on both radars.
2. Tracks should be initialized using three detections, since two detections cause an enormous number of false tracks.
3. Bias correction procedures work when the azimuth bias is less than the normal track correlation region.
4. Typical RMS errors between predicted and measured positions are 0.20 n.mi. and  $0.5^\circ$  for the present filter parameters.
5. The blip-scan ratios of the SPS-12 and SPS-39 are 40% and 50%, respectively. Thus, each radar is supplying about the same number of detections.
6. The turn detector enables the tracking filter to follow maneuvering targets.
7. Detections, not tracks, should be merged. In several instances, a track was maintained with a low blip-scan ratio when neither radar was capable of maintaining an individual track.

Future work for evaluating the system should employ a dedicated aircraft. Tests should be conducted to compare tracking performance (i.e., range error, azimuth error, track duration time, track initiation time, and handoff time) when the data are integrated and when the radars are operating separately. Also, these same tests can be performed in clear and jamming environments.

#### REFERENCES

1. G.V. Trunk, B.H. Cantrell, and F.D. Queen, "Basic System Concept for Integrating a 2D and a 3D Radar and Designs of Automatic Detection System," NRL Report 7678, Mar. 7, 1974.
2. B.H. Cantrell, G.V. Trunk, and J.D. Wilson, "Tracking System for Two Asynchronously Scanning Radars," NRL Report 7841, Dec. 5, 1974.
3. B.H. Cantrell, G.V. Trunk, F.D. Queen, J.D. Wilson, and J.J. Alter, "Automatic Detection and Integrated Tracking System," Int. Radar Conf. Rec., Apr. 1975, pp. 391-395.
4. J.D. Wilson and B.H. Cantrell, "Tracking System for Asynchronously Scanning Radars With New Correlation Techniques and an Adaptive Filter," NRL Report 7952, Jan. 14, 1976.
5. "Program Performance Specification for an AN-SYS-1 Detector/Tracker Sub-System of the DDG2-15 Combat Weapon System," Applied Physics Lab., Johns Hopkins University, XWS-15612, Aug. 1975.
6. G.V. Trunk, B.H. Cantrell, and F.D. Queen, "Modified Generalized Sign Test Processor for 2-D Radar," IEEE Trans. Syst. AES-10, No. 5, 574-582 (1974).
7. L.V. Blake, "Machine Plotting of Radio/Radar Vertical-Plane Coverage Diagrams," NRL Report 7098, June 25, 1970.
8. B.H. Cantrell, "Behavior of  $\alpha$ - $\beta$  Tracker for Maneuvering Targets Under Noise, False Target, and Fade Conditions," NRL Report 7434, Aug. 17, 1972.
9. D.M. White and S.R. Silberman, "Simulation of 2D Radar Automatic Detection and Tracking System: Baseline Program," Technology Service Corp., TSC-W8-60, Aug. 18, 1975.